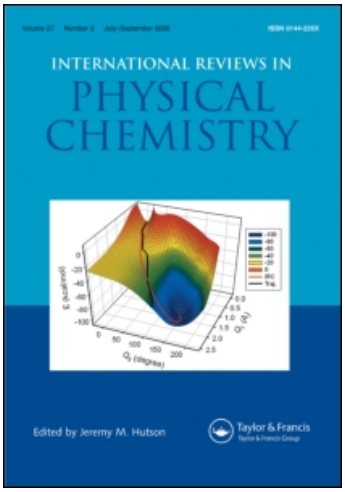

International Reviews in Physical Chemistry
Publication details, including instructions for authors and subscription information:
http://www.informaworld.com/smpp/title~content=t713724383

The dynamics of chlorine-atom reactions with polyatomic organic molecules

Craig Murray[a]; Andrew J. Orr-Ewing[a]
[a] School of Chemistry, University of Bristol, Bristol BS8 1TS, UK

To cite this Article Murray, Craig and Orr-Ewing, Andrew J.(2004) 'The dynamics of chlorine-atom reactions with polyatomic organic molecules', International Reviews in Physical Chemistry, 23: 3, 435 — 482
To link to this Article: DOI: 10.1080/01442350412331329166
URL: http://dx.doi.org/10.1080/01442350412331329166

INT. REVIEWS IN PHYSICAL CHEMISTRY, 2004
VOL. 23, NO. 3, 435–482

Taylor & Francis
Taylor & Francis Group

The dynamics of chlorine-atom reactions with polyatomic organic molecules

CRAIG MURRAY and ANDREW J. ORR-EWING*
School of Chemistry, University of Bristol,
Cantock's Close, Bristol BS8 1TS, UK

Chlorine atoms react with a variety of organic molecules by abstraction of an H atom, making HCl and a radical co-product, and investigations of these reactions provide a large and valuable body of data for improved fundamental understanding of the mechanisms of reactions involving polyatomic molecules. The kinetics and dynamics of reactions of Cl atoms with alkanes have been extensively studied both by experimental and computational methods, and the key outcomes and conclusions are reviewed. These reactions serve as benchmarks for the interpretation of recent experimental data on the dynamics of reactions of Cl atoms with heteroatom functionalized organic molecules such as alcohols, ethers, amines, alkyl halides and thiols. Although bearing many similarities to the dynamics of the alkane reactions, significant differences are found: in particular, the extent of HCl rotational excitation from reactions of Cl atoms with the functionalized molecules is much greater than the very cold rotational distributions obtained for H-atom abstraction from simple alkanes such as methane, ethane, propane and butane. These observations and the scattering dynamics are discussed in terms of reaction energetics, barriers and transition state geometries, and evidence is presented for post-transition-state interactions between the separating HCl and polar organic radical for which the HCl rotation appears to be a sensitive probe.

Contents

*Author to whom correspondence should be addressed. E-mail: a.orr-ewing@bris.ac.uk

International Reviews in Physical Chemistry ISSN 0144–235X print/ISSN 1366–591X online © 2004 Taylor & Francis Ltd
http://www.tandf.co.uk/journals
DOI: 10.1080/01442350412331329166

1. Introduction

At the heart of many bimolecular chemical reactions is the transfer of an atom from one reagent to another, resulting in a change in chemical character. The simplest realization of such atom transfer reactions occurs between an atom and a diatomic molecule, denoted by

$$A + BC \rightarrow AB + C \quad (1)$$

where A, B and C are general labels for the three atoms participating in the reaction. A change in chemical bonding takes place in the transition region between separated reagents and products, with simultaneous breaking of the old BC bond and formation of the new AB bond. Such triatomic systems are attractive to study both experimentally and theoretically for a number of reasons, mostly arising from the small number of degrees of freedom for the motions of the atoms. Within the Born–Oppenheimer approximation, the potential energy of the three-atom system can be described using only three coordinates (typically two interatomic separations and an angle between these two directions), giving a 3D potential energy surface (PES) that controls the motions of the three atoms [1]. Experiments can measure the effects on chemical reactivity and scattering dynamics of energy that is selectively provided to the reagents as collision energy, BC vibrational or rotational energy, and A or BC electronic excitation. The channelling of the excess energy of the reaction into product translation, rotation, vibration and, in some cases, electronic excitation can also be probed using a wide range of sophisticated experimental methods, with the ultimate goal of state-to-state dynamics in which reagents are prepared in a single rovibrational quantum state and products are detected with full quantum-state specificity.

Tremendous progress has been made in the fundamental understanding of chemical reactions from interpretation of the outcomes of reagent-state-selected and product-state-resolved experiments in combination with theoretical and computational advances. In particular, modern theoretical chemistry methods allow calculation of PESs from first-principles quantum mechanics of the interactions between the electrons and nuclei of the various atoms, and either classical or quantum mechanical treatments of the motions of the atoms over the course of a reactive encounter (the reactive scattering) [2, 3]. The outcomes of such calculations can be compared to experimental measurements, enabling refinements of both approaches, and the success of this synergistic strategy is best exemplified by the benchmark reactions $H + H_2 \rightarrow H_2 + H$ (mostly studied using isotopic replacement of one or more H atoms by D atoms) [4], and $F + H_2 \rightarrow HF + H$ [5], for which the

reactive scattering dynamics can now be quantitatively computed at a level matching the best experimental measurements. Fascinating phenomena such as non-adiabatic dynamics (involving switches between adiabatic PESs) [5, 6], and scattering resonances [7–10] have been definitively characterized, and demonstrate that even for an apparently simple atom-transfer reaction as denoted by (1), there is actually immense complexity.

Although the study of reactions of atoms with diatomic molecules has played a pivotal role in the development of current understanding of the fundamental mechanisms and dynamics of chemical reactions, such three-atom processes are not representative of the bulk of chemistry. Many complicated processes, such as hydrocarbon oxidation, either in a flame [11] or in the Earth's troposphere [12], can be reduced to a series of chemical steps involving transfer of one or more atoms, but the transfer may be between polyatomic radicals and molecules. Even chemical transformations on the scale of enzyme-catalysed reactions can involve key reactions with transfer of, for example, an H atom or an H^+ ion [13], and the challenge of modelling the energetics and mechanisms of these various reactions is stimulating much new science. To connect with these fast-developing fields and to provide underpinning, quantitative data that motivate improvements in computational modelling methods, studies of chemical reaction dynamics must tackle polyatomic systems. Moreover, reactions of the type exemplified by (1), but in which either the A or C atom is replaced by a diatomic or polyatomic radical, pose many new questions of fundamental interest that go beyond what is learned from three-atom reaction dynamics. For example, reactions may exhibit multiple, competing pathways, offering the challenge of external (by the scientist) control of the direction of chemical change [14]. Polyatomic reagents and products have vibrational modes of different frequencies and symmetries, involving both stretching and bending motions of the atoms, and thus the effects on reactivity of energizing particular vibrational modes or, in favourable cases, individual bonds, can be explored [15]. Such studies may be confounded by internal vibrational energy redistribution (IVR) on time-scales comparable to, or faster than reaction [16], so careful experimental strategies are needed. Concepts of stereochemistry are widespread in synthetic chemistry, and polyatomic participants in a reaction have shapes, polarities and structures. In addition, reaction may occur at the periphery of a polyatomic molecule, or close to its centre. All these factors will influence the dynamics. Many important questions can also be posed as a result of what has been learned in three-atom reactions, such as the likely importance in polyatomic reactions of scattering resonances, tunnelling dynamics through potential barriers, and non-adiabatic electronic processes.

A move to the study of polyatomic reaction mechanisms and dynamics brings many additional experimental or computational challenges. For example, calculation of scattering dynamics and generation of accurate, fully dimensional PESs become computationally extremely demanding as the number of atoms in a reaction increases beyond three, particularly if several of the atoms are heavy (i.e., not hydrogen) and thus contain numerous electrons. Semi-empirical approaches have been employed: for example, multiple parametrized London–Eyring–Polanyi–Sato (LEPS) functions of the type commonly employed for three-atom reactions, can be combined with additional bending potentials [17]. In certain favourable cases, potential energy points for a large number of configurations of the many-atom system have been computed from *ab initio* electronic structure theory and fitted to obtain global PESs. Other promising strategies, however, that try to reduce the

computational demands, include interpolation methods [18] and direct dynamics calculations in which potential energy points are computed on-the-fly only at required configurations of a scattering calculation [19].

The investment of substantial effort to overcome the challenges posed by polyatomic reactions is unquestionably worthwhile because of the concomitant gains in understanding of chemical reactivity. As alluded to earlier, experiments and calculations can explore many features of polyatomic reactions, including vibrational mode and bond specificity, competition between, and control of, pathways, steric and structural effects, correlations between the rotational and vibrational motions of the two reaction products, and the influence of nearby functional groups on the dynamics. Despite a lack of chemically accurate PESs for many of the reactions to be discussed, much can still be learned and predicted about the dynamics from simple models such as hard-sphere scattering, spectator behaviour, and the requirement for sufficient energy along the line-of-centres of the reacting molecules. As will be discussed later, kinematic constraints arising from the requirements for conservation of linear and angular momentum can be severe in three-atom reactions represented by equation (1), particularly for certain mass combinations of the participant atoms, but the additional degrees of freedom in polyatomic reactions can relax these constraints.

A step-wise strategy for progression from three-atom to polyatom reactions is advantageous, and many researchers have thus elected to conduct experimental or theoretical research on reactions of atomic species with polyatomic molecules. The complexity of a reaction such as that represented by equation (1) is thus increased through replacement of C with a diatomic or larger radical. The main focus of attention has been on model H-atom transfer reactions involving oxygen (either ground-state $O(^3P)$ or the more reactive, electronically excited $O(^1D)$), hydrogen, or halogen atoms. Studies of reactions of $O(^3P)$ with saturated hydrocarbons were recently and comprehensively reviewed by Ausfelder and McKendrick [20].

Abstraction reactions of H atoms from water [21–23] and small alkanes [24, 25] by a further H atom, represented in a general form as

$$H + RH \rightarrow H_2 + R \tag{2}$$

where R is a radical such as OH or CH_3, provide much of the existing experimental dynamical data. In some cases, quantum mechanical calculations of PESs and scattering dynamics are tractable for these reactions. Experiments tend to be performed at high collision energies (perhaps 20–60 kcal mol^{-1}) because the most practical sources of near-monoenergetic H atoms are from ultraviolet laser photolysis of H_2S, HI and HBr, liberating H atoms moving at a few km s^{-1} or faster [26, 27]. The dynamics of these reactions, studied under these high collision energy conditions, are thus somewhat insensitive to the finer details of low-energy regions of the PES. Nevertheless, such reactions have been shown to exhibit surprising bond- and mode-selectivity [21–23].

In this review, we focus on the H-atom abstraction dynamics of reactions of Cl atoms with organic molecules, represented by

$$Cl + RH \rightarrow HCl + R \tag{3}$$

which, as will be argued, are characterized by sensitivity to various interesting features on the PES such as barriers and shallow wells associated with weakly bound pre- and post-transition state complexes. The dynamics of Cl-atom abstraction reactions of H atoms from various classes of organic compounds are described

here, and contrasted with the equivalent, but much more exothermic reactions of F atoms [28–30]. The time-scales for the reactions of these heavy atoms are considerably slower than the equivalent reactions of translationally hot hydrogen atoms, and we will present evidence that slower recoil of the products after H-atom transfer manifests itself in the rotational dynamics of the products. In certain cases, most particularly for reactions with CH_4, high-quality PESs are now available from theoretical calculations, enabling detailed comparisons with experimental data. Laboratory measurements of quantum-state specific scattering for both F and Cl-atom reactions reveal a very rich dynamical behaviour including correlated distributions of the vibrations of both reaction products, rotational and vibrational level dependent scattering, vibrational mode and bond-selective chemistry, and even first evidence for dynamical scattering resonances.

Many of the Cl-atom reactions represented by (3) are of considerable importance in the chemistry of the Earth's atmosphere. It is now well established that Cl atoms react with CH_4 in the stratosphere to form the important reservoir compound HCl, sequestering chlorine and thus inhibiting the catalytic destruction of ozone [12]. Recent progress in studying the chemistry of the troposphere shows that, in the marine boundary layer, Cl_2 release from sea-salt aerosol by oxidation of Cl^- ions, and subsequent solar photolysis to Cl atoms, initiates oxidation chemistry of hydrocarbons similar to that driven by OH radicals, and results in O_3 formation [31]. The chlorine-atom chemistry is estimated to increase ozone mixing ratios over coastal regions of Southern California by up to 12 ppbv (parts per billion by volume), which is highly significant when compared with a global ozone background of between 10 and 40 ppbv. Generation of alkyl radicals by Cl-atom reaction with hydrocarbons is also widely used in laboratory studies to initiate oxidation and thus to study the mechanisms of reactions of great importance in combustion [32].

The reactions of Cl atoms with alkanes are particularly extensively studied and much has been learned over the past decade about the dynamics of reactions of atoms with polyatomic molecules as a consequence of this body of experimental and theoretical work. The greatest effort has concentrated on reactions of methane and ethane with Cl atoms, and these two reactions thus provide benchmark systems against which the dynamics of reactions of other organic molecules can be conveniently compared. We thus start with a review of the key features of the various alkane reactions, highlighting what has been learned from reactions of methane and ethane. Attention is then turned to the reactions of Cl atoms with functionalized organic molecules such as alcohols, ethers, amines and methyl halides to unravel the consequences of the addition of a functional group.

The emphasis of the review will be on reactions of ground electronic state Cl atoms. The lowest energy electronic configuration of a Cl atom is $1s^2 2s^2 2p^6 3s^2 3p^5$, giving rise to two low-lying electronic states, $Cl(^2P_{3/2})$ and $Cl(^2P_{1/2})$, separated by a spin–orbit splitting of 882 cm^{-1} [33], with the $j = 3/2$ state the lower in energy. Most experimental studies of Cl-atom reactions employ $Cl(^2P_{3/2})$ ground-state atoms, which will henceforth be denoted simply as Cl, and thus investigate kinetics and dynamics on the lowest lying PES which correlates adiabatically to the ground electronic states of the reaction products. Certain experiments explore the reactivity of spin–orbit excited $Cl(^2P_{1/2})$ atoms, in particular to investigate non-adiabatic effects during the course of reactions, and these $j = 1/2$ atoms will be distinguished throughout by the widely used notation Cl*. Similar considerations will apply to reactions of $F(^2P_{3/2})$ and $F^*(^2P_{1/2})$ atoms with a spin–orbit splitting of 404 cm^{-1}.

2. Reactions of Cl atoms with alkanes

This section condenses and reviews the existing literature on reactions of Cl atoms with saturated hydrocarbons. Section 2.1 addresses the known kinetics and thermochemistry of a variety of representative reactions, and discussion of the experimental and theoretical studies of the dynamics of the abstraction reactions is contained in section 2.2, including a summary of the effects of vibrational and Cl-atom spin–orbit excitation on reactive scattering.

2.1. *Reaction thermochemistry and kinetics*

Table 1 summarizes the kinetics and thermochemistry of reactions of Cl atoms with selected small saturated hydrocarbons, and figure 1 compares the energetics of selected reactions of Cl and F atoms. Enthalpies of reaction derived from experimental measurements are specified at 298 K, but vary with temperature and thus comparisons with *ab initio* electronic structure theory calculations must be made with caution unless the 0 K calculation results are corrected for temperature effects (or the experimental values corrected to values for 0 K). As can be seen from the error ranges in the enthalpies of reaction, there remain some considerable uncertainties for certain reactions because of poorly specified enthalpies of formation of some of the radical species. In general, however, the abstraction of a primary H atom is clearly less exothermic than abstraction of secondary and tertiary H atoms.

Rates of many of the H-atom abstraction reactions by Cl atoms have been extensively studied over wide temperature ranges because of their importance in atmospheric and oxidation chemistry. The reactions can exhibit non-Arrhenius temperature dependences so activation energies can be difficult to specify. In particular, the reaction of Cl atoms with methane,

$$\mathrm{Cl} + \mathrm{CH_4} \rightarrow \mathrm{HCl} + \mathrm{CH_3} \tag{4}$$

has a temperature dependence of the reaction rate over the range 180–800 K that, when plotted in standard Arrhenius-type form, shows curvature away from Arrhenius behaviour at both the low and high temperature ends of the range. Ravishankara and Wine [34] postulated a significant contribution to the reaction from Cl* atoms at below-ambient temperatures down to 221 K, but Michelsen and Simpson [35] fitted the temperature dependence to the expression

$$k(T) = 2.50^{-1.28}_{+0.71} \times 10^{-12} \left(\frac{T}{298}\right)^{1.27^{+0.68}_{-0.38}} \exp\left(\frac{-\left(938^{-245}_{+135}\right)}{T}\right) \tag{5}$$

and argued, in the light of more recent dynamical data, that the higher temperature (> 298 K) deviation from Arrhenius behaviour could be attributed to the increasing Boltzmann population of excited C–H stretching vibrational modes (the symmetric ν_1 and asymmetric ν_3 stretches) which exhibit faster reaction kinetics than the ground vibrational level. At low temperatures, reaction is enhanced not by spin–orbit excited Cl*, but by tunnelling through the potential barrier, and to a modest extent by low-frequency deformation (often referred to as torsional) and bending modes of the methane. Thus comparison between calculated barrier heights and experimental measurements of activation energies is far from straightforward.

There have been several computational studies of the barrier height and the structure and geometry of the transition state (TS) for reaction of Cl atoms with

Table 1. The thermochemistry and kinetics of reactions of F atoms with methane and Cl atoms with various alkanes. Enthalpies of reaction are at 298 K, and from references [28] and [30] unless otherwise specified. Kinetic parameters are the rate constant, k ($cm^3\,molecule^{-1}\,s^{-1}$), Arrhenius pre-exponential factor, A ($cm^3\,molecule^{-1}\,s^{-1}$), and activation energy, E_a ($kcal\,mol^{-1}$).

Reaction	ΔH_{298}/kcal mol^{-1}	Kinetic parameters/cm^3 molecule^{-1} s^{-1}
$F + CH_4 \rightarrow HF + CH_3$	-31.42 ± 0.21	$k(T) = 1.6 \times 10^{-10} \exp(-260/T)$ $k(298\,K) = 6.7 \times 10^{-11}$ [29, 30] ($E_a = 0.52\,kcal\,mol^{-1}$)
$Cl + CH_4 \rightarrow HCl + CH_3$	$+1.82 \pm 0.10$	$k(T) = 6.6 \times 10^{-12} \exp(-1240/T)$ from 200–300 K [29, 30] $k(298\,K) = 1.0 \times 10^{-13}$ $A = 6.6 \times 10^{-12}$ ($E_a = 2.7\,kcal\,mol^{-1}$ [(a)])
$Cl + CD_4 \rightarrow DCl + CD_3$	$+2.7 \pm 0.10$ [98]	$k(298\,K) = 8.2 \pm 1.0 \times 10^{-15}$ [118] ($E_a = 3.9\,kcal\,mol^{-1}$)
$Cl + C_2H_6 \rightarrow HCl + C_2H_5$	-2.08 ± 0.39	$k(298\,K) = 5.9 \times 10^{-11}$ [29, 30] $A = 8.6 \times 10^{-11}$ ($E_a = 0.27 \pm 0.05\,kcal\,mol^{-1}$ [45])
$Cl + C_2D_6 \rightarrow DCl + C_2D_5$	-0.25 [98]	$k(295\,K) = 8.30 \pm 0.7 \times 10^{-12}$ [176] ($E_a = 0.75\,kcal\,mol^{-1}$ [98])
$Cl + C_3H_8 \rightarrow HCl + n\text{-}C_3H_7$	-2.77 ± 0.60	This and the next channel were not distinguished in kinetics experiments.
$Cl + C_3H_8 \rightarrow HCl + i\text{-}C_3H_7$	-4.57 ± 0.39	$k(298\,K) = 1.38 \pm 0.03 \times 10^{-10}$ [29, 30] independent of T [45].
$Cl + c\text{-}C_3H_6 \rightarrow HCl + c\text{-}C_3H_5$	-3.10 ± 0.25 [49]	$k(T) = (1.8 \pm 0.3) \times 10^{-10} \exp(-(2150 \pm 100)/T)$ $k(296\,K) = 1.15 \pm 0.17 \times 10^{-13}$ [50]
$Cl + i\text{-}C_4H_{10} \rightarrow HCl + i\text{-}C_4H_9$	-2.01 (0 K) [80]	$k(T) = 8.52 \times 10^{-11} \exp(-(292 \pm 6)/T)$ [47]
$Cl + i\text{-}C_4H_{10} \rightarrow HCl + t\text{-}C_4H_9$	-7.03 (0 K) [80]	$k(T) = 2.89 \times 10^{-11} \exp(-(138 \pm 10)/T)$ [47]
$Cl + n\text{-}C_4H_{10} \rightarrow HCl + C_4H_9$	-2.01 ± 0.50 (0 K) for abstraction of a 1° H	$k(298\,K) = 2.2 \times 10^{-10}$ independent of T [29]
	-5.52 ± 0.50 (0 K) for abstraction of a 2° H	$k(298\,K) = 2.05 \times 10^{-10}$ [30]
$Cl + n\text{-}C_5H_{12} \rightarrow HCl + C_5H_{11}$	-2.0 for abstraction of a 1° H -5.4 for abstraction of a 2° H [83]	$k(296\,K) = 2.51 \times 10^{-10}$ [48]
$Cl + c\text{-}C_6D_{12} \rightarrow DCl + c\text{-}C_6D_{11}$	-8.0 ± 2.0 (at 0 K) [61]	$k(294\,K) = (1.3 \pm 0.5) \times 10^{-10}$ [61]

(a) E_a is difficult to specify because of curvature in the Arrhenius plot (see text for a discussion).

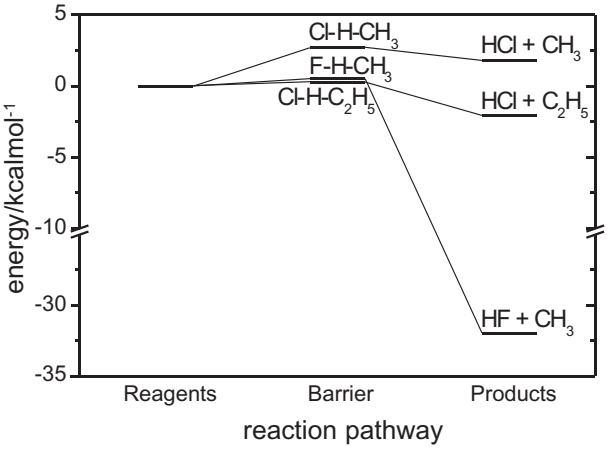

Figure 1. Reaction energetics for the $Cl + CH_4$, $Cl + C_2H_6$ and $F + CH_4$ reactions specified at 298 K. Barrier heights are derived from temperature-dependent kinetic studies.

methane. The Cl−H−C group is unarguably collinear in the minimum energy geometry of the TS (which thus has C_{3v} symmetry), and the TS occurs late on the reaction coordinate, but obtaining a correct value of the barrier height is challenging and requires careful treatment of electron correlation effects. Donahue and co-workers proposed a model in which the barrier height for this and other radical–molecule reactions is determined by the energy gap to the lowest ionic PES [36]. In early calculations, Truong *et al.* [37] used second- and fourth-order Møller–Plesset perturbation theory methods (MP2 and MP4) with a variety of basis sets and obtained a best estimate of the forward barrier height of 7.9 kcal mol^{-1}. Inclusion of zero-point energies corrects this value to a vibrationally adiabatic barrier height of 3.5 kcal mol^{-1} and a reaction endothermicity (at 0 K) of 1.2 kcal mol^{-1}, both in good accord with experimental data. Dobbs and Dixon [38] overestimated the activation energy by > 1 kcal mol^{-1} at the MP2 level with a triple-zeta basis set, so obtained computed reaction rates that were significantly too low. Their density functional theory (DFT) calculations, on the other hand, returned a barrier that was much too low when corrected for zero-point energy effects.

Despite the computational challenge, potential energy surfaces have been calculated for reaction (3), some incorporating the full dimensionality of the six-atom system [17, 39–41] and variational transition state theory (VTST) used to compute temperature-dependent rate constants that show impressive levels of agreement with experimental data [39, 42, 43]. Troya *et al.* [43], for example, obtained rate constants over the temperature range 200–500 K using high-level *ab initio* potential energies along the minimum energy pathway for reaction. Unrestricted second-order Møller–Plesset perturbation theory (UMP2), with a 6–311G(2df, 2pd) basis set was used for geometry optimizations and harmonic frequency calculations of stationary points and connecting pathways, and the energies recalculated using spin projected unrestricted fourth-order Møller–Plesset perturbation theory (PUMP4) with the same basis set. An *ab initio* energy barrier of 2.83 kcal mol^{-1} (including zero-point energy corrections) was obtained that compares very favourably with the experimental activation energy of $\sim$2.7 kcal mol^{-1} (see Table 1). VTST calculations with tunnelling corrections gave rate constants that are in excellent agreement with recommended experimental values: for example,

at 300 K the experimental and computed values are 1.0×10^{-13} and 1.1×10^{-13} cm^3 molecule^{-1} s^{-1}, respectively. Calculations by Duncan and Truong [42, 44] of vibrationally selected reaction rates showed that excitation of the CH_4 symmetric stretch vibrational mode enhanced the H-atom transfer rate, and a low-frequency umbrella-type vibration also promoted reaction. HCl vibration promoted the reverse reaction, but the CH_3 ν_2 umbrella vibration, which might also be judged to be along the reaction coordinate, had an inhibiting effect. These conclusions are supported by subsequent calculations [39, 40].

Recent experimental studies from Taatjes and co-workers [45], and a body of experimental data incorporated in tables of recommended kinetic parameters by Atkinson *et al.* [28–30], show straightforward Arrhenius-type temperature dependence of the rate constant for reaction of Cl atoms with ethane (reaction (6) below) over the range 292–600 K (with some curvature for 600–800 K) and evidence for a very low barrier to reaction. These studies and compilations report no temperature dependence, and thus no significant barrier for reaction of Cl atoms with propane (reactions (7a) and (7b), which cannot be distinguished in the kinetics experiments) over the range 292–700 K. Sarzynzki and Sztuba [46], however, observed a weak temperature dependence for reactions (7a) and (7b), with respective activation energies of 0.14 ± 0.03 and -0.21 ± 0.06 kcal mol^{-1}. The negative value was attributed to formation of a very weakly bound complex, and reaction of Cl atoms with *n*-butane exhibited similar Arrhenius behaviour. The activation energies for abstraction of a primary and the tertiary H atom from *i*-C_4H_{10} were reported to be 0.58 ± 0.01 kcal mol^{-1} and 0.27 ± 0.02 kcal mol^{-1}, respectively [47]. No temperature dependence has been reported for the Cl + *n*-C_5H_{12} reaction, although the reaction is rapid [48].

$$Cl + C_2H_6 \rightarrow HCl + C_2H_5 \tag{6}$$

$$Cl + C_3H_8 \rightarrow HCl + n\text{–}C_3H_7 \quad (CH_2CH_2CH_3) \tag{7a}$$

$$\rightarrow HCl + i\text{–}C_3H_7 \quad (CH_3CHCH_3) \tag{7b}$$

By way of contrast, the endothermic reaction [49] of Cl atoms with cyclopropane, which forms the cyclopropyl radical

$$Cl + c\text{–}C_3H_6 \rightarrow HCl + c\text{–}C_3H_5 \tag{8}$$

shows a temperature-dependent rate with a deduced activation energy of 4.3 ± 0.2 kcal mol^{-1} [50].

Computational studies of the energetics and kinetics of reactions of Cl atoms with alkanes other than methane remain scarce. *Ab initio* calculations of the transition state structures and activation energies of the reactions of various halogen atoms with ethane and propane [51] at levels of theory up to MP4 with a 6–31G(d) basis set show near-collinear X–H–C groups in the transition state (X = F, Cl or Br). Barrier heights are, however, overestimated. VTST and kinetic isotope effect (KIE) calculations for the ethane reaction have been undertaken using dual level *ab initio* methods [52, 53]. A small but non-negligible barrier to reaction is found from experiments, but the *ab initio* calculations struggle to reproduce this: for example, MP4/cc–pVTZ level calculations give a negative activation energy of $E_a = -0.1$ kcal mol^{-1} [53]. The exothermicity of the reaction is, however, well duplicated by the calculations, and rate constants were derived

that were within a factor of 2.6 of those measured experimentally. Computational studies of the dynamics of some of these reactions will be discussed later.

Taatjes and co-workers also investigated the temperature-dependent rates of reaction of Cl atoms with some selected unsaturated hydrocarbons. Propene ($CH_3CH=CH_2$) reaction with Cl exhibits simple Arrhenius behaviour at temperatures from 400 to 800 K, with direct abstraction of an H atom, but at temperatures below 400 K there is clear evidence of adduct formation [54]. Ethene ($CH_2=CH_2$) reacts with a Cl atom at room temperature and below via addition to form a chloroethyl radical, with HCl produced by a secondary reaction [55]. Above 500 K, however, direct abstraction of an H atom dominates. Reaction of Cl with allene ($CH_2=C=CH_2$) for $T = 292$–850 K shows an addition mechanism at low T (to form the resonance stabilized chloroallyl radical) that switches to direct HCl formation via abstraction at higher temperature, with an HCl yield of unity at 800 K [56]. Reaction with the isomeric molecule propyne ($HC\equiv CCH_3$) occurs by competing addition and abstraction mechanisms, with abstraction dominating at temperatures above 500 K. This review will, however, concentrate on the dynamics of reactions of the saturated hydrocarbons, rather than be diverted by the interesting addition and elimination pathways observed for some of the unsaturated molecules.

It is particularly noteworthy that, of the usual saturated hydrocarbons (methane, ethane, propane, butane, etc.) only methane exhibits a significant activation barrier in its reaction with Cl atoms, and it is the only endothermic reaction. This distinction makes the methane reaction somewhat atypical, and will be an important consideration in the comparisons of dynamics of reactions of alkanes and functionalized organic molecules with chlorine atoms in subsequent sections.

For the purposes of comparison, we consider briefly the equivalent reactions of F atoms with alkanes. A striking feature, as illustrated in figure 1, is that the F-atom reactions are all much more exothermic than the near-thermoneutral Cl + alkane reactions because of the energy gained from formation of the strong HF bond [28, 29]. Transition states thus tend to be earlier along the reaction coordinate and the excess energy of the reaction is channelled very efficiently into vibrational excitation of the nascent HF. Thus, for example, Kim and Setser [57] monitored IR emission from HF from reaction of F atoms with a series of cyclic alkanes from cyclohexane to cyclodecane. The HF was formed mostly in $v = 2$, with 50% of the available energy converted to HF vibration.

2.2. *Reaction dynamics*

The dynamics of H-atom abstraction reactions of Cl atoms with alkanes show a richness and diversity that is, on first encounter, quite baffling. Careful study by several groups over the last decade has, however, highlighted some useful trends and simplified models that can account for most of the experimental observations in an intuitive and satisfying manner. As such, the dynamics of these reactions provide valuable benchmarks against which other polyatomic molecule reactions can be compared.

For reactions of C_3 and higher non-cyclic alkanes there are competing pathways for abstraction of primary (1°), secondary (2°) and perhaps tertiary (3°) H atoms. The thermochemistry of these different channels is illustrated in Table 1 for propane, *n*-butane, *i*-butane and *n*-heptane. Partial deuteration of the alkane, and measurement of HCl and DCl reaction products, can be used to deduce the relative reactivities of H (or D) atoms bonded in different (1°, 2° or 3°) environments within

the alkane. With correction for the number of available H or D atoms at a particular site in a target molecule, the central, 2° H atoms in propane were estimated to be 2.7 ± 0.4 times more reactive than terminal, 1° H atoms despite the latter being more exposed to approach of Cl atoms [58, 59]. Similarly the HCl-to-DCl ratio of 3.3 ± 0.4 for reaction of Cl atoms with the mono-deuterated *t*-butane $(CH_3)_3CD$ demonstrates a 2.7-fold greater reactivity of the individual 3° D atom when corrected for the 9-to-1 statistical ratio of sites [60].

2.2.1. *Rotational distributions of the HCl products of Cl + alkane reactions*

The first experiments that measured the nascent rotational excitation of products of a Cl-atom reaction with an alkane were carried out by Flynn and co-workers [61], who used diode laser absorption to monitor the DCl ($v' = 0$, J') products of the reaction with perdeuterated cyclohexane:

$$Cl + C_6D_{12} \rightarrow DCl + C_6D_{11} \tag{9}$$

Two collision energy regimes were employed, with mean values of 5.3 and 14.3 kcal mol^{-1} in the centre-of-mass (CM) frame, and 95% of the DCl was estimated to be formed in its vibrational ground state. Very little of the available energy (only 2%) was, on average, channelled into DCl rotation, with the bulk of the energy partitioned between product translation and internal excitation of the C_6D_{11} radical. The fraction of the available energy becoming internal energy of this radical, f_{int}, was determined to be 0.60 and 0.37 at the two respective collision energies of 5.3 and 14.3 kcal mol^{-1}. Efficient mapping of increasing collision energy into product translation, as was observed, is typical of the constrained kinematics of reactions such as (9) in which a light atom is transferred between two heavy particles. The C_6D_{11} radical was argued to behave like a spectator, making little or no contribution to the scattering dynamics, but accounting for some considerable fraction of the available energy either because of reorganization of the structure of the C_6D_{11} framework after loss of a D atom from the equilibrium geometry of C_6D_{12} (an idea further developed by Suits and co-workers [62] to interpret their data on O(^{3}P)-atom reactions with alkanes) or through statistical excitation of the 45 vibrational modes. This latter suggestion was deemed unlikely for a direct abstraction reaction. Most puzzling was the observation that the DCl products were very rotationally cold, because this observation strongly implies a near-collinear Cl−D−C geometry during the recoil of the DCl: any deviation from collinearity would result in a torque about the DCl centre of mass, and thus DCl rotational excitation. Similar arguments were proposed by Andresen and Luntz [63, 64] to account for the very rotationally cold OH radicals observed in reactions of O(^{3}P) with a variety of alkanes. Such a constrained geometry, most probably enforced by a steeply rising potential energy for geometries deviating from the collinear minimum energy path, is hard to reconcile with the large reaction rate constant (see Table 1), and thus low activation energy and large Arrhenius *A*-factor which imply few geometrical constraints in the transition region and a 'loose' transition state. Flynn and co-workers proposed that rotational reorientation of the C_6D_{12} on approach of Cl, to ensure collinear attack at a D−C bond, would be too slow, but that large-amplitude zero-point bending vibrational motion of a D atom might successfully bring the Cl into a head-on geometry with the D−C bond. The apparent contradiction between low rotational excitation of DCl or HCl reaction products and kinetic measurements, as well as broad angular scattering distributions observed

in more recent experiments (*vide infra*), is a recurring theme in the reactions of Cl atoms with alkanes.

Innovative experimental approaches employed by Zare and co-workers [65–74] have played a very important part in developing a deep understanding of the dynamics of reactions of Cl atoms with small alkanes, both by making observations that ran contrary to the received wisdom at the time, and by stimulating numerous theoretical studies. The extensive programme of study over the past 12 years in Zare's group was initiated by some ground-breaking experiments by Simpson *et al.* [65–69] in which CH_4 was prepared vibrationally excited with one quantum of the triply degenerate asymmetric stretch mode, ν_3, using the infrared beam from an optical parametric oscillator (OPO). Cl atoms were generated by UV photolysis of Cl_2 that was co-expanded with the methane through a small orifice in a pulsed nozzle into a high-vacuum chamber. The nascent HCl molecules formed from the state-to-state reaction

$$Cl + CH_4(\nu_3 = 1,\ J) \rightarrow HCl(v'J') + CH_3 \tag{10}$$

were quantum-state specifically probed by resonance enhanced multiphoton ionization (REMPI), with the HCl^+ ions detected within a time-of-flight mass spectrometer (TOF–MS). The so-called 'photoloc' method, developed independently by Shafer *et al.* [75] and by Brouard and co-workers [76], was used to derive CM frame differential cross-sections (DCSs) by analysis of the laboratory frame velocity distributions of the HCl molecules (which determine the arrival times of the HCl^+ ions at the detector of the TOF–MS, and thus the shapes and widths of the TOF profiles). Simpson *et al.* measured HCl rotational level population distributions for both $v' = 0$ and 1 reaction products, and, most surprisingly, observed that despite being very rotationally cold, the HCl ($v' = 1$, $J' = 0$–3) products exhibited pronounced *forward* scattering in the CM frame [65, 68, 69]. This observation was at odds with the widely accepted arguments of Andresen and Luntz [63, 64], put forward in the context of reactions of $O(^3P)$ with alkanes, that low rotational excitation of the diatomic product following an H-atom abstraction reaction must be indicative of a collinear moiety in the transition state of the reaction, and thus should be associated with *backward* scattering in the CM frame. The HCl ($v' = 0$, J') products of reaction (10) were indeed formed mostly backward-scattered, but the CM frame DCSs for HCl ($v' = 1$, J') also exhibited some dependence on the rotational level of the HCl, with more pronounced forward scatter for the lower J' levels, and an increasing component of backward scatter for $J' = 3$. Higher J' levels were only weakly produced in the reaction.

The observation of forward scatter for the HCl ($v' = 1$, J') products is an example of a phenomenon that is increasingly observed in quantum-state resolved experiments of forward scattering for the thermoneutral channel (i.e., the channel in which there is little or no change in the kinetic energies of the reactants through to the products, so any energy release from the reaction appears as internal energy of the products). By aligning the CH_4 (or CD_3H) vibrations in the laboratory frame using polarized IR excitation, Simpson *et al.* [68] were able to demonstrate that the reactions leading to forward scattering were occurring for side-on attack of Cl atoms at a C–H bond at large impact parameters, corresponding to reaction at the periphery of the target molecule [77]. Stripping of the H atom barely perturbed the forward trajectory of the Cl atom, so kinetic energy was largely conserved and

a non-impulsive transfer of the H atom was suggested to account for the low HCl rotation. Lower impact parameters were associated with more backward-scattered products and the greater impulse required to turn around the heavy HCl molecule in the CM frame could thus explain the greater rotational excitation of the back-scattered HCl. These studies prompted many further experiments on the dynamics of Cl-atom reactions with small alkanes, and DCSs have now been reported for the reactions of Cl atoms with ethane [70–73, 78], propane [79], butane [80–82], and pentane [83]. Where HCl rotational level-dependent DCSs have been extracted, the higher J' products show greater backward scattering, consistent with the arguments presented above.

In all the reactions studied so far of Cl atoms with saturated hydrocarbons, the HCl (or DCl) products are observed to form with *very low degrees of rotational excitation*. REMPI detection schemes require careful calibration to convert nascent spectral line intensities to relative populations of quantum states, but this is routinely achieved by recording spectra of room-temperature HCl, which is, of course, randomly distributed over m_J states (i.e., not aligned or oriented). The results of three independent experimental studies are shown in figure 2 for reaction (4) of Cl atoms with methane (not prepared vibrationally excited) [69, 80, 84], and figure 3 shows the outcomes of measurements for reactions of a series of different hydrocarbons. In Table 2, the data are summarized as mean rotational energies and rotational temperatures obtained from Boltzmann plots of the rotational population distributions. There is some correlation of rotational energy with increasing exothermicity of the reaction, as is apparent, for example, for 1° versus 2° H-atom abstraction [82]; nevertheless the conversion of available energy from the reaction into rotational excitation of the HCl is extremely inefficient, typically corresponding to fractions of less than 0.04 (with reaction of Cl atoms with methane the exception because of the much smaller available energy for this endothermic process). The dynamics thus appear to be similar to the analogous H-atom abstraction reactions of $O(^3P)$ atoms with alkanes [20, 63], for which the OH

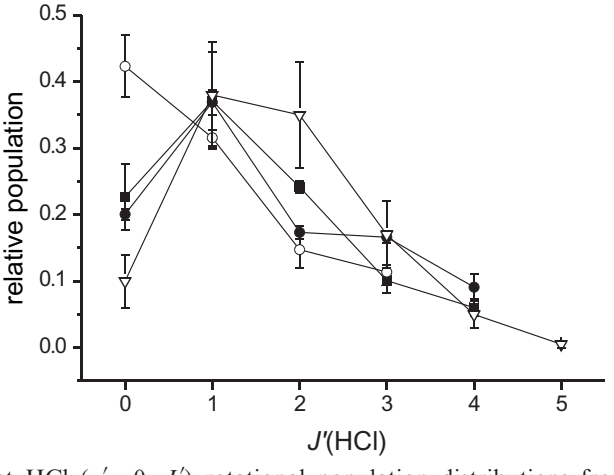

Figure 2. Nascent HCl ($v'=0$, J') rotational population distributions from the $Cl+CH_4$ reaction measured experimentally by Murray *et al.* (■) [84], Simpson *et al.* (○) [69] and Varley and Dagdigian (●) [80]. Also shown are the results of reduced dimensionality QCT calculations performed by Troya *et al.* (▽) [43].

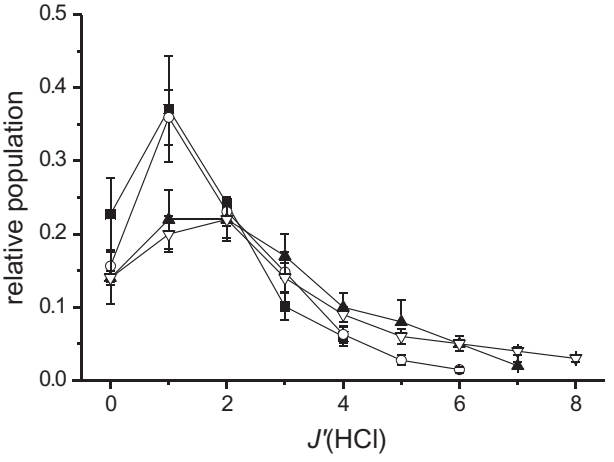

Figure 3. Nascent HCl ($v' = 0$, J') rotational population distributions for the reactions of Cl atoms with the alkane series methane (■) [84], ethane (○) [152], propane(▲) [80], and butane (▽) [80].

Table 2. Mean rotational energies, rotational temperatures and rotational fractions of the total available energy for HCl products of reactions of Cl atoms with alkanes at mean collision energies $\langle E_{coll} \rangle$, specified in units of cm^{-1} for ease of comparison with the HCl rotational energies.

Reaction	$\langle E_{coll} \rangle$ /cm^{-1}	$\langle E_{rot} \rangle$ /cm^{-1}	T_{rot} /K	f_{rot}	Reference
$Cl + CH_4 \rightarrow HCl + CH_3$	1295	64 ± 4	88 ± 6	0.093	84
$Cl + C_2H_6 \rightarrow HCl + C_2H_5$	1895	69 ± 5	117 ± 5	0.023	152
$Cl + n\text{-}C_3H_8 \rightarrow HCl + C_3H_7$	3760	117		0.024	80
$Cl + i\text{-}C_4H_{10} \rightarrow HCl + C_4H_9$	4100	175		0.034	80
$Cl + n\text{-}C_4H_{10} \rightarrow HCl + n\text{-}C_4H_9$	2580	60		0.02	82
$\rightarrow HCl + s\text{-}C_4H_9$		170		0.04	82

radical products are invariably formed rotationally cold, but the inference by Andresen and Luntz [63, 64], supported experimentally by Suits and co-workers [62] using crossed molecular beam and velocity map imaging methods (but somewhat at odds with results of Tsurumaki *et al.* [85]), of backward-scattered products, does not apply to the Cl-atom reactions, as will be demonstrated below.

A number of models exist for analysis and interpretation of rotational distributions, largely based on statistical treatments [1], kinematic constraints, or classical, impulsive dynamics [86–91]. Statistical treatments apply if there is formation of a reaction complex long-enough lived for statistical redistribution of energy and angular momentum, and thus a well on the PES is required. For hydrogen-atom transfer between two heavier atoms, conservation of angular momentum arguments demonstrate a kinematic tendency for the orbital angular momentum of the reagents (**L**) to be largely conserved in the products (i.e., $\mathbf{L} \rightarrow \mathbf{L}'$), but tell us little about the rotational angular momenta of the two products. If impulsive models are used to try to account for the very low rotational excitation of the HCl, then, because of the transfer of a light atom between two relatively heavy particles, the torque about the centre of mass of the newly forming HCl will be

large unless the deviation of the Cl–H–C moiety away from collinearity is very small. Indeed, impulsive models predict that the ∠Cl–H–C angle must be no greater than a few degrees away from 180° for the reaction of Cl atoms with CH_4 to account for HCl formed predominantly in $J' = 0$, 1 and 2. Valentini and co-workers [92] have considered further the consequences of the mass combination for such reactions (termed a heavy + light–heavy, or $H + LH$ system) on the maximum fraction of the available energy that can be channelled into internal excitation of the reaction products, using a simplified model of reflection of trajectories from the inner repulsive wall of the appropriate PES. If the PES is plotted in mass-weighted coordinates [1] the skew angles for $H + LH$ systems are small, and there are strong constraints on the rotational excitation of the HCl. Although the model is overly simplistic in treating such reactions as pseudo-triatomic systems, with neglect of the internal degrees of freedom of the radical co-product, it does moderately successfully predict the maximum rotational quantum number of the HCl that can be formed from reaction of Cl atoms with CH_4 ($J'_{max} = 3$) and C_2H_6 ($J'_{max} = 9$). What it does not do, however, is account for the distribution of J' values up to this maximum, and thus does not explain on kinematic grounds alone the very low rotational excitation of the HCl.

2.2.2. *Scattering dynamics and differential cross-sections*

The DCSs measured for the reaction of Cl atoms with ground-state methane are strikingly different from those reported for reactions of Cl atoms with other alkanes. Independent measurements for reaction of Cl atoms with CH_4 and CD_4 by Zare and co-workers [74], Vallance and co-workers [93], and definitive imaging studies from Liu and co-workers (see figure 4) [94], show that the DCl products of reaction of Cl with CD_4 are strongly backward-scattered, indicating rebound-type dynamics, and that reaction with CH_4 leads to HCl also scattered into the backward hemisphere but in a more sideways direction. These are to be contrasted with the results for vibrationally excited methane [65, 66, 68] in which a forward scattering

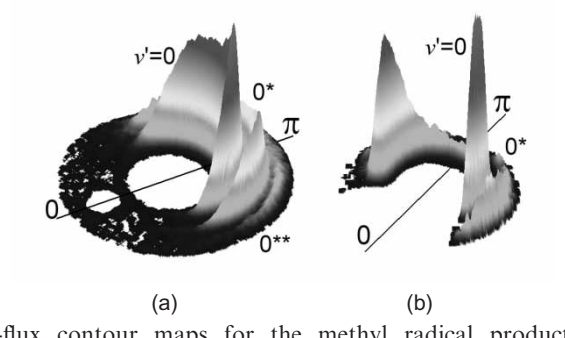

Figure 4. Velocity-flux contour maps for the methyl radical products of reactions of Cl atoms with (a) CD_4 at a collision energy of 4.78 kcal mol^{-1} and (b) CH_4 at a collision energy of 4.60 kcal mol^{-1}. The angular coordinate shows the CM-frame scattering angle, with 0 and π radians, respectively, corresponding to forward and backward scattering of the methyl radical. The radial coordinate is the methyl radical speed in the CM frame. Structures labelled as 0, 0* and 0** correspond, respectively, to CD_3 or CH_3 moving at speeds consistent with formation from CD_4 or CH_4 in its vibrational ground state ($v = 0$), $v_4 = 1$ or $v_4 = 2$ levels. The figure is adapted from ref. [94].

channel was observed, as described earlier. Many of the outcomes of these experiments can be tied together within an overall picture for the dynamics of Cl-atom abstraction of H atoms from saturated hydrocarbons that draws on relatively simple models. The scattering distributions can be successfully accounted for using a hard-sphere scattering model, in which low impact parameter collisions lead to backward and side scattering, coupled with a requirement for sufficient collision energy along the line-of-centres to surmount the collinearly favoured barrier to reaction. Using a combination of these models, Simpson *et al*. [69] were able to map the ranges of impact parameters for Cl-atom reaction with CH_4 that lead successfully to reaction, and showed how vibrational excitation of the CH_4 results in an opening up of the range of successful impact parameters, with a shell of large impact parameters giving the forward scattered HCl ($v' = 1$) products. This semi-quantitative analysis of the data is consistent with the notion of peripheral reaction dynamics leading to forward scattered products in cases when there is not a significant barrier to reaction.

The scattering dynamics is remarkably well treated using a combination of hard-sphere scattering and line-of-centres models [1] of the reactive collision, as first showed by Simpson *et al*. [69] and adapted by Kim *et al*. [95] to incorporate translational energy release. In essence, collision of two hard spherical particles occurs at a distance d that is the sum of their radii, and the scattering angle, θ, is determined by the impact parameter, b, according to:

$$\cos\theta = \frac{2b^2}{d^2} - 1 \tag{11}$$

Large values of b (tending to d), and thus glancing or 'peripheral' collisions, are thus seen to be necessary to give forward scatter. Approach of the two particles with total translational energy E_T and a centre-to-centre separation R at non-zero impact parameter results in some of the available energy becoming centrifugal energy ($E_T b^2/R^2$), and the total available energy must exceed a threshold to reaction, E_0, that is the sum of the potential energy barrier and the centrifugal energy barrier. The model supposes that this threshold occurs at distance $R = d$ and the kinetic energy along the line-of-centres that can be used to surmount this threshold barrier is the total kinetic energy minus the centrifugal energy, $E_T(1 - b^2/d^2)$. This condition places a maximum value on the impact parameter beyond which the threshold energy cannot be overcome, of:

$$b_{\max} = d\left(1 - \frac{E_0}{E_T}\right)^{1/2} \tag{12}$$

The correlation between impact parameter and scattering angle, (11), means that such constraints on b will map into restrictions on the DCS. For a simple opacity function $P(b)$ describing the reaction probability as a function of the impact parameter, that is constant up to a maximum b and zero beyond, the hard-sphere and line-of-centres models predict a differential cross-section $d\sigma/d\cos\theta$ that is uniform from backward scattering ($\cos\theta = -1$) up to a maximum value of $\cos\theta$ given by

$$(\cos\theta)_{\max} = 1 - \frac{2E_0}{E_T} \tag{13}$$

beyond which the DCS is zero. Note that the maximum scattering angle depends upon the collision energy.

Although very simple, the model does surprisingly well, for example predicting cut-offs in the scattering angle for $Cl + CH_4$ and $Cl + CD_4$ of, respectively, cos $\theta_{max} = -0.5$ and -0.8 that are in reasonable accord with experiments. The line of centres is, however, less clearly defined for collisions of non-spherical particles: for methane we can take the line between the Cl and C atoms, but for reaction with ethane and larger hydrocarbons, we might choose the CM of the molecule, or the C atom at which H-atom abstraction takes place. A further important point about the model is that if the H atom is transferred along the line between the Cl and C atoms, which will be close to the direction of transfer of momentum, there will be no torque and the HCl will form rotationally cold. The critical geometry for reaction will thus correspond closely with the minimum energy geometry for the TS for $Cl + CH_4$ (or $Cl + C_2H_6$) as obtained from *ab initio* calculations.

Incorporation of repulsive energy release into this model modifies the outcomes somewhat but also provides important insights [95]. If δE is the kinetic energy release associated with an impulse at the point of contact of two hard spheres, there will be an associated deflection of the relative velocity of the two particles that results in a minimum scattering angle away from the forward direction ($\theta = 0^\circ$) such that cos θ takes a maximum value that depends upon the ratio $\delta E/E$, where E is the initial kinetic energy. Thus even glancing collisions close to the maximum impact parameter will be deflected away from the fully forward scattering direction by impulsive energy release. For a thermoneutral channel, with $\delta E = 0$ and thus no change in the kinetic energy over the course of the reaction, equation (13) applies and the near thermoneutral reaction can give fully forward scatter, but as the impulsive energy release increases, larger deflection angles result in more backward scattering of the reaction products. The model thus rationalizes the experimental observation that, when reaction can occur over a wide range of impact parameters (when there is no significant barrier to reaction), forward scattering is generally associated with the thermoneutral products such as $Cl + CH_4$ ($\nu_3 = 1$) $\rightarrow$ HCl ($v' = 1$) + CH_3 ($v' = 0$), whereas more backward-scattered products are observed for the channels with greater kinetic energy release, such as $Cl + CH_4$ ($\nu_3 = 1$) $\rightarrow$ HCl ($v' = 0$) + CH_3 ($v' = 0$).

Qualitative application of the hard-sphere scattering and line-of-centres models of the scattering dynamics also does well in describing the outcomes of measurements of DCSs for the reaction of Cl atoms with ethane. In this case (as well as for reaction of Cl atoms with higher alkanes [80, 81, 82]), as illustrated in figure 5, much broader angular distributions of HCl are observed than for $Cl + CH_4$, with an increasing propensity for backward scatter for the small fraction of reaction products formed in HCl rotational levels from $J' = 6$ to $J' = 8$ [70, 78]. The majority of products are formed in $J' = 0$–3 and exhibit broad scattering that is forward peaking. The key difference for ethane (and higher alkanes) as compared to the methane reaction (4) is that the latter reaction has a relatively high barrier (estimated to be 2.7 kcal mol^{-1}); the reactions of Cl atoms with higher alkanes are all known to have much smaller or non-existent barriers. The line-of-centres model thus puts much greater constraints on the impact parameters for attack of Cl atoms at methane than for the other reaction systems, resulting in less forward scatter. An angle-dependent barrier height also enforces tighter restrictions on the attack angle at an H–C bond; in the jargon of the dynamical stereochemistry community,

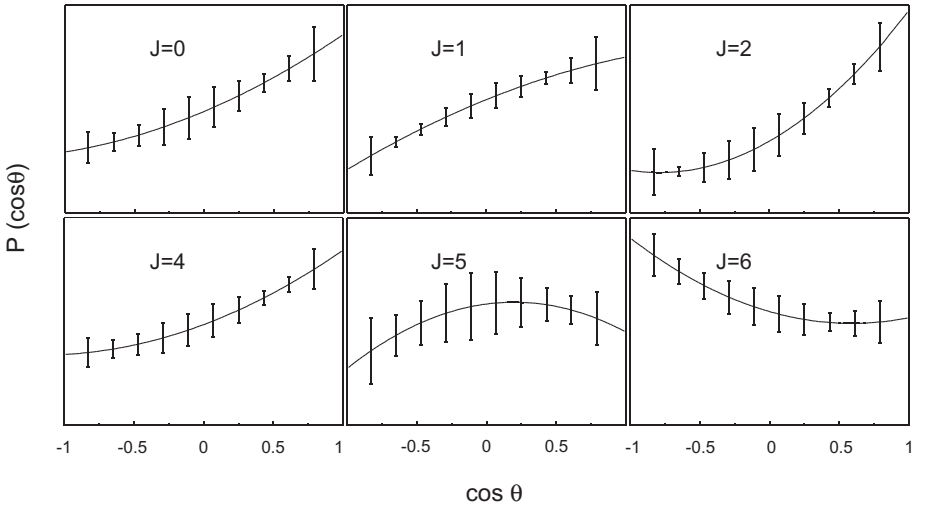

Figure 5. State-resolved CM-frame angular distributions for the HCl ($v' = 0$, J') products of the $Cl + C_2H_6$ reaction performed at a collision energy of 5.4 kcal mol^{-1}. The figure is adapted from ref. [82].

this is referred to as a tighter cone of acceptance for approach of the Cl atoms to methane for successful reaction [96]. In the barrierless or near-barrierless reactions of Cl atoms with other alkanes, a cone of acceptance with a very wide opening angle leads to reaction at a broad range of impact parameters and thus broad scattering in the CM frame. There are few, if any steric constraints on the approach of the Cl atom and thus a molecule such as ethane appears chemically as a ball of H atoms any one of which can be abstracted either by Cl atom attack straight-on or side-on to a C–H bond. C–H stretching vibrational excitation of the C_2H_6 molecule thus barely affects the reaction probability or the scattering dynamics (only weakly enhancing formation of HCl in J' states greater than 3) despite the $\sim$3000 cm^{-1} greater internal energy of one reagent [71], unlike reaction (10) in which the internal excitation of the CH_4 enhances reactivity by a factor of $\sim$30 and opens up forward scattering dynamics. One interpretation of this latter result is that the internal excitation of the CH_4 essentially eliminates the barrier to reaction characteristic of the methane system, and thus the vibrationally excited methane behaves dynamically much more like ethane and higher alkanes in its reactions with chlorine atoms.

2.2.3. *HCl/DCl rotational alignment*

Further insight into the mechanisms of hydrogen-atom transfer comes from measurements of the scattering-angle dependence of the spatial alignment of the rotational angular momentum [97] of the DCl products of reaction of Cl atoms with CD_4 (at a collision energy $E_{coll} = 6.5$ kcal mol^{-1}) and C_2D_6 ($E_{coll} = 5.8$ kcal mol^{-1}) [98]. In the former reaction, the DCl product rotational angular momentum was found to be maximally aligned perpendicular to its recoil velocity in the CM frame, indicating a late transfer of the D atom, whereas for reaction with C_2D_6, half-maximal alignment perpendicular to the line-of-centres direction was interpreted as evidence of earlier D-atom transfer, near to the distance of closest approach of the Cl atom. The conclusions for the CD_4 reaction were supported by quasi-classical trajectory calculations on an empirical and reduced

dimensionality PES that confirm the experimental observation and interpretation, and argue for transfer of the D atom close to the plane containing the relative velocity vectors of reagents and products [99]. In contrast, for reaction of CH_4 ($\nu_3 = 1$), the positive rotational alignment of the forward scattered HCl products was interpreted as indicative of *out-of-plane* transfer of the H atom at large impact parameters [100], with J' generated perpendicular to the line-of-centres. Again, simplified QCT calculations were able to reproduce the experimental observations [101].

2.2.4. *Internal energies of the radical products of reactions of Cl + alkanes*

Experiments have probed not just the properties of the HCl products, but have also determined the internal energies of the radical co-products of the abstraction reactions, either by direct spectroscopic measurement (in the case of the CH_3 radical, via REMPI detection) or by energy conservation arguments following determination of the translational energy release. In the reactions of Cl with CH_4 and CD_4, little or no excitation of the CH_3/CD_3 radical is observed ($\sim$2.3% CH_3 ($\nu_2 = 1$) and $\sim$3% CD_3 ($\nu_2 = 1$) [74]) despite relaxation of a pyramidal CH_3 (or CD_3) geometry in the Cl–H–CH_3 transition state to a planar minimum energy geometry of the methyl radical. This geometry change might be expected to excite one or more quanta of the low-frequency ν_2 umbrella vibration of the methyl, but instead adiabatic relaxation to the vibrational ground state of the radical appears to occur, perhaps reflecting a non-impulsive release of the energy of the reaction. For reaction of Cl with ethane, measurements by Kandel *et al.* [70] appeared consistent with only a small amount of internal energy deposition into the ethyl radical, but more recent experiments and re-analysis by Bass *et al.* [78] suggest a fraction $f_{int} = 0.22$ of the available energy becoming internal motion of the C_2H_5. By analogy with the geometry change for the methyl radical, some of this energy might be expected to reside within umbrella-type wagging of the CH_2 group in the ethyl radical, but trajectory calculations by Rudić *et al.* [19] suggest strongly that most of the energy becomes rotation of the ethyl radical simply because of the torque induced on it during transfer of an H atom, with the line of force (the Cl–H–C axis) offset from the centre of mass of the ethyl radical. Model calculations that assume impulsive energy release support the idea of rotational excitation of the C_2H_5 [78]. If, as predicted by the trajectory calculations, the rotational angular momentum quantum number of the ethyl radical can, on average, be $J'_{ethyl} \sim 20$–30, kinematic constraints imposed by total angular momentum conservation will be considerably relaxed because the angular momentum of the products is partitioned between rotational motion of the two products as well as orbital motion.

For reaction of Cl atoms with propane [79] and *n*-pentane [83] at higher collision energies than those typical of the methane and ethane experiments, Suits and co-workers attributed a forward scattered component in the DCS with large KE release to abstraction of a 2° H atom (the more exothermic channel, with a lower barrier) whereas slower moving, backward and sideways scattered products were assigned to reaction involving a 1° H atom. This analysis is consistent with a line-of-centres argument that the channel with the greater, though still modest, barrier is constrained to smaller impact parameters and thus more rebound-like dynamics. The data have, however, been subjected to recent reinvestigation because the method used (vacuum ultraviolet photoionization of the alkyl radical) might favour detection of vibrationally excited radicals [82, 102]. Bass *et al.* [82], in experimental

studies of the reaction of Cl atoms with *n*-butane, report contrary observation of forward scattered HCl in low rotational levels from peripheral abstraction of a 1° H atom, and more rotationally excited HCl (up to $J' = 6$) from reaction at 2° sites that is near-isotropically scattered in the CM frame because of reaction at a wide range of impact parameters. For both pathways, internal excitation of the *n*-butyl ($52 \pm 6\%$ branching) or *s*-butyl ($48 \pm 6\%$) radical product accounts for a fraction of 0.29 of the available energy. A significant part of this internal energy is likely to be in rotation according to impulsive energy release models, but excitation of some of the numerous low-frequency vibrational modes of the butyl radical is also probable. For abstraction of a 1°H atom from *n*-pentane, the balance of the energy was suggested to become vibrational excitation of the C_5H_{11} 1-pentyl radical [83], which has numerous low-frequency modes. Substantial rotation of the radical was rejected, however, for the back-scattered 1° H-atom abstraction products because the large impact parameter of the reagents (*b*, defined relative to the CM of the long pentane molecule) is conserved into the impact parameter (b') of the separating products. Conservation of orbital angular momentum, in part determined by the value of *b* or b', was thus suggested to preclude substantial rotational angular momentum of the 1-pentyl radical, but this argument overlooks the fact that the direction of the orbital angular momentum is reversed for back-scattered products and, in fact, the 1-pentyl radical must rotate to conserve overall angular momentum (as one would expect macroscopically for a long rod struck impulsively at one end).

2.2.5. *Reactions of vibrationally excited CH_4*

Vibrational excitation of CH_4 is now well-known to enhance its reactivity with Cl atoms: in a line-of-centres type model, the cone of acceptance for approach of Cl is opened up by vibrational excitation because the effective barrier to reaction is reduced, so the reaction cross-section increases [69]. The first demonstration of this effect estimated a ~30-fold enhancement in the yield of HCl at a collision energy of $3.7\,\mathrm{kcal\,mol^{-1}}$ if the CH_4 is prepared with one quantum of the asymmetric C–H stretch vibration, ν_3. Crim and co-workers [103] subsequently compared the enhancements in reactivity of the two C–H stretching vibrational modes ν_1 (the symmetric stretch) and ν_3 through excitation of the near isoenergetic CH_4 ($\nu_1 + \nu_4$) and ($\nu_3 + \nu_4$) stretch–bend combination bands, both of which are IR active in CH_4 (the ν_1 band alone is not IR active, but can be excited by stimulated Raman pumping, SRP). The ($\nu_1 + \nu_4$) excited CH_4 was found to be ~2 × more reactive than the CH_4 ($\nu_3 + \nu_4$), and to have a reaction cross-section ~ 20 × greater than ground or thermally populated CH_4 vibrational levels. The origin of the greater reactivity of the symmetric stretch excited mode was proposed, by analogy with calculations on the $Cl + H_2O$ reaction [104] and for scattering of methane at a nickel surface [105], to arise from adiabatic localization of the stretching vibrational energy within the C–H bond proximal to the approaching Cl, whereas the asymmetric stretch vibration localizes in a non-reactive, distal C–H bond. This proposition was further supported by experiments and calculations on the reaction of Cl atoms with CH_3D prepared with one quantum of symmetric or asymmetric C–H stretching vibration, with the former exhibiting 7-fold more efficient enhancement of reaction [106]. Intriguingly, however, Bechtel *et al.* [107] have recently shown that CH_4 ($\nu_3 = 1$) and CH_4 ($\nu_1 = 1$) (the latter prepared by SRP) in reaction with Cl atoms at a collision energy of $\sim 3.7\,\mathrm{kcal\,mol^{-1}}$ exhibit indistinguishable reaction dynamics: the HCl rovibrational population distributions and the DCSs for the two reactions are identical within

experimental uncertainties, and the intensity patterns within the CH_3 REMPI spectra also appear to be equivalent. These observations suggest that the reaction of vibrationally excited methane involves a single C–H oscillator, with the relative phases of the other C–H oscillators inconsequential to the reaction dynamics.

From the now numerous studies of reactions of vibrationally excited methane and partially deuterated methanes with Cl atoms, two further conclusions stand out. The first is that these systems exhibit bond selective chemistry, so, for example, stretching vibrational excitation of a C–H bond in CHD_3 results in predominant formation of $HCl + CD_3$ reaction products, as first noted by Simpson *et al.* [68]. Further compelling evidence for bond specificity in related reactions comes from the work of Kim *et al.* [108], Bechtel *et al.* [109], and Yoon *et al.* [110], and is largely a consequence of local mode type C–H and C–D stretching vibrations in the various partially deuterated isotopomers of methane. The second particularly noteworthy outcome is that vibrational excitation in the non-reactive part of the methane molecule is efficiently conserved into the product methyl radical, indicating weak coupling to the reaction coordinate and spectator-like behaviour. For example, for the reaction [108]:

$$Cl + CH_2D_2|1100\rangle \rightarrow HCl + CHD_2 \tag{14}$$

with the local mode description of the vibrations, $|v_a v_b v_c v_d\rangle$ denoting the number of vibrational quanta in each of the two C–H bonds (v_a and v_b) and the two C–D bonds (v_c and v_d), the CHD_2 is observed to form with vibrational excitation in the retained C–H bond. In contrast, the reaction

$$Cl + CH_2D_2|2000\rangle \rightarrow HCl + CHD_2 \tag{15}$$

with very similar vibrational energy in the CH_2D_2, forms CHD_2 with no detected vibrational excitation in the C–H or C–D stretches.

HCl ($v = 0$) formed from reaction of vibrationally excited CH_4 ($\nu_3 = 1$) is rotationally hotter than from Cl-atom reactions with other, ground vibrational state, alkanes [69, 107], with a mean rotational energy of 0.86 kcal mol^{-1} (300 cm^{-1}). This pathway is exothermic by 6.7 kcal mol^{-1} and, with inclusion of the collision energy, rotational excitation of HCl corresponds to a fraction of 0.08 of the available energy. There is thus a hint that greater exothermicity corresponds to greater impulsive energy release and so greater HCl rotation. Such arguments are not, however, clear-cut because for CH_4 prepared with *two* quanta of C–H stretch vibrational excitation (one quantum in each of two C–H bonds), the HCl products are formed rotationally cold despite apparent repulsive energy release [95]. For

$$Cl + CH_4(\nu_3 = 2; |1100\rangle) \rightarrow HCl + CH_3 \tag{16}$$

the major channels to form HCl ($v = 1$) + CH_3 ($\nu_2 = 1$) and HCl ($v = 0$) + CH_3 (ν_1 or $\nu_3 = 1$) are exothermic by ~4.9 and 6.6 kcal mol^{-1}, and there is additional collision energy amounting to 3.4 kcal mol^{-1}, yet respective mean energies in HCl rotation are only 0.23 and 0.61 kcal mol^{-1} (i.e., fractions of the available energy of 0.03 and 0.06). Kim *et al.* [95] successfully demonstrated the use of a hard-sphere and line-of-centres model, modified to incorporate repulsive energy release, to describe the DCSs for these channels, and argued that transfer of the H atom, together with impulsive energy release, was thus along the line of centres between the Cl and the C atom thereby inhibiting any torque from bent Cl–H–C geometries that might map into HCl rotation.

There is some controversy about the extent of enhancement of reaction of Cl atoms with methane thermally excited in low-frequency deformation (ν_2) or bending (ν_4) vibrations; the two cannot usually be distinguished in experiments because they lie very close in energy. Kandel and Zare [74] were first to show that at collision energies close to the threshold, CH_4 or CD_4 (ν_2 or $\nu_4 = 1$) weakly populated in a pulsed expansion because of inefficient vibrational cooling of a thermal sample, are responsible for HCl or DCl formation with laboratory frame speeds energetically inaccessible to the reaction of vibrationally ground-state CH_4 or CD_4. These authors estimated that at collision energies of $3.0\,\mathrm{kcal\,mol^{-1}}$ the vibrationally excited CH_4 (ν_2 or $\nu_4 = 1$) is 400 times more reactive than CH_4 ($v = 0$), and this ratio reduces to 200 times for a collision energy of $5.5\,\mathrm{kcal\,mol^{-1}}$. Enhancement of reaction by these low-frequency modes is qualitatively consistent with predictions from theoretical calculations of their effects on reaction rates [42, 44]. Subsequent experiments and data analysis have confirmed the contribution to reaction of the methane excited in low-frequency vibrational modes [35, 93, 94, 111] but these later studies suggest a much lower enhancement factor. The very recent imaging experiments of Liu and co-workers [94] have sufficient resolution to distinguish CH_3 radicals formed from CH_4 ($v = 0$) and CH_4(ν_2 or $\nu_4 = 1$), and their results suggest that it is the bending mode ν_4 that is responsible for the most energetic CH_3 fragments, but with a reactivity enhancement only of a factor of 3. The equivalent extra energy in translation would be more efficient at promoting reaction, implying a non-mode-specific effect. The imaging experiments, with their unprecedented product kinetic energy resolution, appear clear-cut, and reasons for the discrepancies with the enhancement factors of Kandel and Zare [74] remain moot, but may originate from an underestimate of the width of the distribution of collision energies.

2.2.6. *Reaction of Cl* with alkanes*

The possible reaction of spin–orbit excited Cl* atoms with CH_4 is an interesting dynamical question because, much as for reaction of Cl* with H_2, formation of ground electronic state products can only occur following non-adiabatic transitions from excited PESs correlating with electronically excited products. The adiabatic correlations are illustrated schematically in figure 6. Non-adiabatic transitions are suspected to occur in the entrance valley of the PES, before the transition state is reached, or in close proximity to the TS. Marked discrepancies persist between theoretical [6] and experimental [112] measurements of the relative reactivities of Cl and Cl* towards H_2, with non-adiabatic quantum scattering calculations predicting a much lower Cl* reactivity than is reported experimentally, in contrast to the excellent agreement between experiment and theory for the reactivities of F and F* with H_2 [5, 113—116]. Recent investigations of the dynamics of the Cl reaction with CH_4 near the energetic threshold show no evidence for a contribution to reaction from Cl* [94], [117]; indeed, kinetics studies suggest that the Cl* is quenched to Cl about 300× faster than reaction of Cl with CH_4 so deactivation will be the major process [118]. A more fruitful place to look for dynamical consequences of Cl* chemistry might be in reactions with larger alkanes because Matsumi and co-workers [119] showed the rate of reaction of Cl* with propane and *n*- and *i*-butane to make HCl to be ~30% of that of ground spin–orbit state Cl atoms.

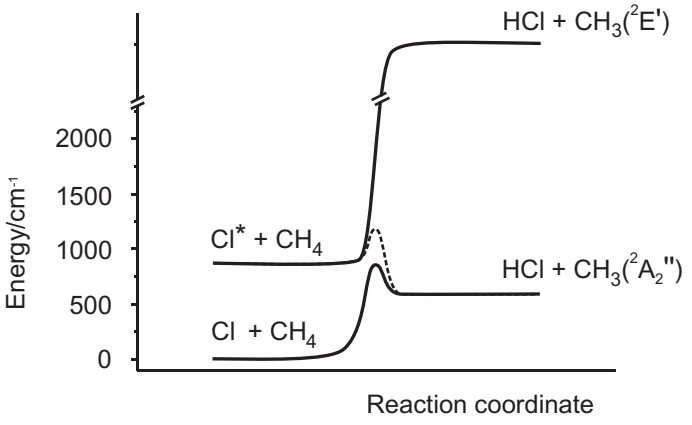

Figure 6. Schematic adiabatic reaction profiles (solid lines) for the reaction of CH_4 with ground Cl and spin–orbit excited Cl* atoms. Cl* atoms correlate with the energetically forbidden $HCl + CH_3(^2E')$ products asymptote, therefore can only react via non-adiabatic transfer (dashed line with a schematic barrier) onto the ground-state surface.

2.2.7. *Computational studies of the dynamics of Cl-atom reactions with alkanes*

There is a rich and growing literature on computational studies of the dynamics of reactions of Cl atoms with methane, using both quasi-classical and quantum scattering dynamics on potential energy surfaces, with dimensionality ranging from pseudo-three-atom systems (with the CH_3 treated as a single particle of mass 15) up to the full treatment of all six atoms. There are many fewer computational studies of reaction of Cl atoms with ethane [120], but Rudić *et al.* [19] recently demonstrated that rather than generating a global PES, direct dynamic techniques, with solution of the classical equations of motion using potential energy points and forces computed on-the-fly at the geometries sampled by the trajectories, is a very promising approach that can successfully account for much of the experimentally observed data for these larger systems. The trajectories can also be used to generate animations of reactive encounters that show the behaviour of all the participating atoms and thus provide a clear visualization of the dynamics. Representative trajectories can be viewed on a website at the University of Bristol [121].

Most of the reduced dimensionality calculations of the dynamics of the $Cl + CH_4$ reaction suppose, with support from experimental measurements described earlier, that the CH_3 group is only weakly coupled to the reaction coordinate and thus can be treated as a single particle. Levine and co-workers [17] carried out QCT calculations for reaction of vibrationally excited CH_4 ($\nu_3 = 1$) on LEPS-function based PESs using such a 3D model and compared the outcomes with 4D (incorporating the CH_3 umbrella bending vibration) and full six-atom dynamics. Problems with correct treatment of the zero-point energy complicated the latter two calculations, but many qualitative features of the experimental measurements were retrieved and the authors concluded that the major features of the dynamics were insensitive to the level of description of the CH_3, in accord with the experimental observations of spectator-like behaviour of the methyl. The trajectories confirmed the connection between impact parameters and scattering angles of the HCl deduced from hard-sphere scattering models. Forward scatter was, however, attributed to

formation of an 'osculating' complex surviving for about half a rotational period of the transition state.

The most comprehensive comparisons of QCT calculations (of reduced dimensionality) with experiment come from Troya *et al*. [43] for reaction of Cl atoms with vibrational ground-state and vibrationally excited CH_4 using a high-level *ab initio* PES fitted to an analytical function and reduced to 3D atom + pseudo-diatomic molecule coordinates. The excellent agreement of the outcomes of the dynamics calculations with several experimental measurements, such as HCl rotational population distributions (as shown in figure 2) and quantum-state resolved differential cross-sections, implies that the approximation that the CH_3 modes are only weakly coupled to the reaction coordinate is a good one for this reaction. Methane C–H stretching vibrational excitation was, however, calculated to increase the reaction cross-section only by a factor of 4, rather than the factor of 30 ± 15 derived from experiments, but does enhance the HCl product rotation because trajectories can access more repulsive regions of the PES. Direct dynamics trajectory calculations with *ab initio* potential energies and forces computed on the fly have also recently proved successful in describing certain features of the reactive scattering [19], and hold considerable promise for future development, particularly if fast semi-empirical potential energy calculations of sufficient accuracy can be exploited.

Nyman and co-workers have steadily developed quantum mechanical scattering methods to treat the reaction of Cl atoms with methane [122–125], evolving from 2D to 4D, with the 3D and 4D calculations reproducing many key features of the thermal kinetics, kinetic isotope effects, and the reaction dynamics, including preferred scattering directions. The effect of bend excitation in methane on the extent of HCl rotation has also been examined quantum mechanically [126].

3. Reactions of F atoms with alkanes

It is beyond the scope of this article to delve deeply into the dynamics of reactions of F atoms with alkanes, but some brief comparisons are very instructive. Much effort has focused on the reaction

$$F + CH_4 \rightarrow HF + CH_3 \qquad (17)$$

the kinetics and thermodynamics of which are summarized in Table 1. Most notable, in comparison with the equivalent reaction of Cl atoms with methane, is that the F-atom reaction is considerably more exothermic (largely a consequence of the heat of formation of HF) [28, 29], with a much lower activation barrier and higher rate constant. Troya *et al*. [127] calculate a linear F–H–C configuration (i.e., C_{3v} symmetry) for the minimum-energy saddle-point structure at a variety of different levels of theory, apparently correcting an F–H–C bend angle of 161.2° obtained in previous UMP2 calculations with a smaller (6–31G(d,p)) basis set [128].

Dynamical measurements of outstanding quality by Lin and co-workers [129–133] reveal correlated HF and CH_3 vibrational distributions, and quantum-state resolved DCSs from crossed molecular beam experiments that are reminiscent of vibrationally resolved reactive scattering of F with H_2, HD and D_2 [134, 135]. The HF from reaction (17) is formed in vibrational levels up to $v' = 3$ at the energies of the experiments, and exhibits a vibrational inversion because of dynamics on an attractive PES with an early barrier and substantial exothermicity. Very recent measurements of the collision energy dependence of the state-resolved scattering

provide tantalizing evidence for a scattering resonance [132, 135], much as has been reported (and recently definitively assigned) for the reaction of F with HD [8–10, 136, 137]. Unlike the $F + H_2/HD$ reaction, however, there is a linear geometry at the transition state (for the F–H–C moiety).

Nesbitt and co-workers [138, 139] studied reaction (17) under crossed molecular beam conditions (with very well-defined collision energies) and obtained nascent HF rotational (J') and vibrational (v') level population distributions via thorough IR laser absorption measurements, together with information on the scattering from analysis of Doppler widths. The measured relative vibrational populations were 0.106(3) in $v' = 3$; 0.667(14) in $v' = 2$; 0.189(27) in $v' = 1$ and 0.038(78) in $v' = 0$, with the numbers in parentheses providing uncertainties on the last digits. The HF ($v' = 1$) rotational level populations fit to a mean rotational energy of 1450 cm^{-1} (4.2 kcal mol^{-1}) that is considerably hotter than the HCl formed from any of the Cl + alkane reactions, most plausibly because of greater repulsive energy release from the transition state. Rotational levels in $v' = 2$ and 3 are also populated up to, or near the energetic limit. An impulsive energy release model also accounts well for the internal energy of the C_2H_5 fragments formed from the reaction of F atoms with ethane [140]: for a given HF (v', J') product, the energy partitioned to the ethyl radical, which constitutes $> 70\%$ of the available energy, is divided approximately equally between translational and internal motions, and experimental data are consistent with a Franck–Condon type excitation of the CH_2 wagging vibration.

The dynamics of the reaction of F atoms with methane have received some theoretical attention, most noteworthy of which are QCT calculations by Troya *et al.* [127] on an *ab initio* but reduced dimensionality PES (with the CH_3 treated as a single particle) and by Kornweitz *et al.* [141] on a six-atom empirical PES. The neglect of methyl radical internal degrees of freedom is challenged by diode laser absorption experiments [142] and recent velocity map imaging results of Lin and co-workers [129–133] that show vibrational excitation of the umbrella mode that increases with collision energy, providing further evidence of greater repulsive energy release along the F–H–C coordinate than for Cl-atom reaction with methane. Despite this concern, however, the dynamics of the newly formed HF are well-reproduced by both sets of trajectory calculations, with greater forward scattering as the HF vibrational quantum number increases, and HF ($v = 3$) (the thermoneutral channel) formed by grazing collisions at large impact parameter.

4. Reactions of Cl atoms with functionalized organic molecules

In this section we review the current literature describing experimental and theoretical studies of the dynamics of H-atom abstraction reactions between Cl atoms and functionalized organic molecules. Such studies have a shorter history than the equivalent reactions of alkanes, and the reactions have received far less scrutiny either experimentally or computationally, but rapid progress has occurred in recent years to include the reactions of alcohols, ethers, amines and methyl halides, which will be the main focus of this section. We discuss the kinetics and thermochemistry of the reactions which have been the subjects of dynamics studies in section 4.1, and focus on the dynamics in section 4.2, drawing comparisons with the benchmark Cl-atom reactions with small alkanes and highlighting some key differences.

Table 3. The thermochemistry and kinetics of reactions of Cl atoms with various functionalized organic molecules. Enthalpies of reaction are at 298 K, and from references [28], [30] and [144] unless otherwise specified. Kinetic parameters are the rate constant, k (cm^3 $molecule^{-1}$ s^{-1}), Arrhenius pre-exponential factor, A (cm^3 $molecule^{-1}$ s^{-1}), and activation energy, E_a (kcal mol^{-1}).

Reaction	ΔH_{298} /kcal mol^{-1}	Kinetic parameters/ cm^3 $molecule^{-1}$ s^{-1}
$Cl + CH_3F \rightarrow HCl + CH_2F$	-3.06 ± 2.01	$k = 3.5 \times 10^{-13}$; $A = 1.7 \times 10^{-11}$ ($E_a = 2.3 \pm 1.0$ kcal mol^{-1})
$Cl + CH_3Cl \rightarrow HCl + CH_2Cl$	-2.35 ± 1.02	$k = 4.9 \times 10^{-13}$; $A = 3.3 \times 10^{-11}$ ($E_a = 2.5 \pm 0.6$ kcal mol^{-1})
$Cl + CH_3Br \rightarrow HCl + CH_2Br$	-1.55 ± 1.05	$k = 4.4 \pm 10^{-13}$; $A = 1.02 \pm 10^{-15}$ $T^{1.42}$; fit to modified Arrhenius expression ($E_a = 1.3$ kcal mol^{-1}) [155]
$Cl + CH_3I \rightarrow HCl + CH_2I$	0.55 ± 1.62	$k = 8.2 \times 10^{-13}$; $A = 5.44 \times 10^{-11}$ ($E_a = 2.5 \pm 0.2$ kcal mol^{-1}) [156]
$Cl + CH_3OH \rightarrow HCl + CH_2OH$	-7.12 ± 0.32	$k = 5.5 \times 10^{-11}$, no T dependence
$\rightarrow HCl + CH_3O$		
$Cl + CH_3CH_2OH \rightarrow HCl + CH_3CHOH$	-10.13 ± 1.01	$k = 9.0 \times 10^{-11}$, no T dependence
$\rightarrow HCl + CH_2CH_2OH$		
$\rightarrow HCl + CH_3CH_2O$		
$Cl + CH_3OCH_3 \rightarrow HCl + CH_2OCH_3$	-10.1	$k = 1.3 \times 10^{-10}$
$Cl + CH_3NH_2 \rightarrow HCl + CH_2NH_2$	-10.0	Unreported
$\rightarrow HCl + CH_3NH$	-3.3	
$Cl + CH_3SH \rightarrow HCl + CH_2SH$	-10.0	$k = 4.3 \times 10^{-12}$ [167]
$\rightarrow HCl + CH_3S$	-15.8 ± 0.46	$k = 2.0 \times 10^{-10}$; $A = 1.2 \times 10^{-10}$, with a negative temperature dependence

4.1. *Reaction thermochemistry, kinetics, and site-specific branching*

The kinetics and thermochemistry of the reactions of Cl atoms with functionalized organic molecules are summarized in Table 3. As with the reactions of Cl atoms with saturated hydrocarbons, the primary uncertainties in the enthalpies arise from the uncertainties in the heats of formation of the organic radical products. In some cases, the discrepancy between the NASA and IUPAC recommendations for atmospheric chemistry is over 1 kcal mol^{-1} [143, 144]. With the exception of the methyl halides, abstraction from a methyl group adjacent to a heteroatom is generally more exothermic than abstraction of a primary H atom from a methyl group in a hydrocarbon (typically -2 to -3 kcal mol^{-1}).

Kinetic studies of the reactions of Cl atoms with oxygenated molecules are less extensive than those of the corresponding alkanes, and remain a subject of active current investigation, largely because of environmental concerns. Typically, the reactions of small alcohols and ethers are rapid and have been found to be effectively independent of temperature, where investigated. Of the oxygenated molecules listed in Table 3, dimethyl ether (DME) reacts most rapidly with Cl atoms, having a rate constant approaching the limiting gas kinetic value, and results exclusively in HCl and the CH_3OCH_2 radical. The temperature dependence of the rate constant has been reported only once, in a flash photolysis-resonance fluorescence experiment by

Michael *et al.* [145] and was found to be invariant over the range 200–500 K. The reaction between Cl atoms and methanol is known, at least at ambient temperatures, to proceed almost entirely (> 95%) via the more exothermic methyl H abstraction channel to produce the hydroxymethyl radical [146]:

$$Cl + CH_3OH \rightarrow HCl + CH_2OH \quad \text{branching} > 0.95 \tag{18a}$$

$$\rightarrow HCl + CH_3O \quad \text{branching} < 0.05 \tag{18b}$$

This reaction is also rapid and temperature-independent, indicating that any barrier to reaction at the methyl group is either non-existent or negligibly small [145]. Jodkowski *et al.* [147] performed *ab initio* calculations at the G2 level of theory to calculate the energies of stationary points on the PES for the $Cl + CH_3OH$ reaction and found no barrier to the production of the hydroxymethyl radical, while a significant barrier of $8.1\,kcal\,mol^{-1}$ was computed for reaction at the hydroxyl site. Additionally, weakly bound pre- and post-reaction molecular complexes were located and it was argued that the reaction proceeded via these complexes. Rate constant calculations suggested that the methoxy-producing channel was insignificant below 1000 K. Recent diffusion Monte Carlo (DMC) calculation for reaction (18a), however, compute a $2.39 \pm 0.49\,kcal\,mol^{-1}$ barrier and enthalpies of reaction of $-6.99 \pm 0.49\,kcal\,mol^{-1}$ and $-5.82 \pm 0.50\,kcal\,mol^{-1}$, at 0 K and 298 K, respectively [148]. Smith *et al.* [149] used IR laser absorption to measure the absolute rate constant for the reaction between Cl atoms and methanol at 295 K and determined a branching fraction of 12% for production of vibrationally excited HCl. In a very recent kinetic study, Seakins *et al.* [150] determined the vibrational branching fraction for HCl ($v' = 1$) products of reaction (18a) to be 25% at 298 K, decreasing slightly to 22% at 243 K, although both values were within the mutual uncertainties. The discrepancy between the measurements is curious, given the good agreement for the vibrational branching in the $Cl + CH_3CH_2OH$ reaction discussed below.

The reaction of Cl atoms with ethanol can proceed exothermically via abstraction of primary or secondary H atoms (at the β and α positions) to produce 2-hydroxyethyl and 1-hydroxyethyl radicals, respectively, the latter pathway being more energetically favoured:

$$Cl + CH_3CH_2OH \rightarrow HCl + CH_3CHOH \quad \text{branching} \sim 0.92 \tag{19a}$$

$$\rightarrow HCl + CH_2CH_2OH \quad \text{branching} \sim 0.08 \tag{19b}$$

$$\rightarrow HCl + CH_3CH_2O \quad \text{branching negligible} \tag{19c}$$

As in the $Cl + CH_3OH$ reaction, abstraction of the hydroxyl H atom to give HCl and the ethoxy radical is mildly exothermic but inhibited by a significant barrier. Taatjes *et al.* [151] measured absolute and site-specific rate coefficients for the reaction of Cl atoms with selectively deuterated ethanol isotopomers over the 295–600 K temperature range using time-resolved IR absorption spectroscopy of the HCl products and total product analysis using FTIR spectroscopy in a smog chamber. The negligible HCl yield from the reaction of $Cl + CD_3CD_2OH$ highlighted the lack of reactivity of hydroxyl H atoms to Cl attack. Only slight temperature dependences were observed for the reactions of all the isotopomers, and Arrhenius fits to the rate coefficients for formation of HCl products from the $Cl + CH_3CH_2OH$ and $Cl + CD_3CH_2OH$ reactions showed negative activation energies, indicating barrierless abstraction of an α-hydrogen. The activation energy

derived for the $Cl + CH_3CD_2OH$ reaction, however, was found to be small and later *ab initio* calculations revealed a 0.73 kcal mol^{-1} barrier to this weakly exothermic channel [152]. The branching fractions for β-hydrogen abstraction determined from both experimental approaches were in excellent agreement, revealing that about 8% of the HCl products are formed *via* this channel at 296 K. A branching fraction for production of vibrationally excited HCl products of around 20% for the products of the $Cl + CH_3CH_2OH$ reaction was reported by both Taatjes *et al*. [151] and by the more recent study of Seakins *et al*. [150].

With the exception of the $Cl + CH_3I$ reaction, which is thought to be slightly endothermic (but within the uncertainties, could be exothermic), the hydrogen abstraction reactions of Cl atoms with the methyl halides (CH_3X)

$$Cl + CH_3X \rightarrow HCl + CH_2X \quad X = F, Cl, Br, I \tag{20}$$

are mildly exothermic and the enthalpies of reaction are comparable to those for abstraction of primary H atoms from alkanes other than methane, although subject to uncertainties of the order of $\sim$ 1–2 kcal mol^{-1}. For the reactions of Cl atoms with CH_3Br and CH_3I, halogen substitution to form CH_3Cl and Br or I atoms has been observed [153], but only as a minor pathway, and crossed beam scattering experiments have also investigated the alternative, endothermic, ICl-producing abstraction channel of the latter reaction [154]. Kinetics studies showed the H abstraction channel to be the dominant pathway under atmospheric conditions [155, 156]. The room temperature rates of the H abstraction reactions of Cl atoms with the methyl halides are significantly (one to two orders of magnitude) slower than the reactions with the oxygenated molecules discussed earlier [143, 144]. Arrhenius expressions describing the temperature dependence of the kinetics show small A parameters, and activation energies similar to the $Cl + CH_4$ reaction. Theoretical work on the kinetics of the reactions is limited. Rayez *et al*. [157] characterized the geometries of the transition states (at the MP2/6–31G(d,p) level) for the reactions of Cl atoms with a series of fluoro- and chloro-substituted methanes and applied transition state theory with a one-dimensional tunnelling correction to calculate the room temperature rate constants. With the inclusion of the tunnelling correction the calculated rate constant for the $Cl + CH_3F$ reaction was approximately a factor of three smaller than the experimental value, and the agreement was worse for the $Cl + CH_3Cl$ reaction. Rosenman and McKee [158] optimized the transition state geometries for the $Cl + CH_3F$ reaction at the MP2/6–31 + G(d) level, as well as several points along the minimum energy pathway. Variational TST rate constants were calculated over the temperature range 200–700 K, and were in generally good agreement with the experimental values when zero-curvature tunnelling was included, except at the lowest temperatures. Xiao *et al*. [159] have also investigated the kinetics of the $Cl + CH_3Cl$ and CH_3Br reactions theoretically. Using optimized transition states and intrinsic reaction coordinate calculations of the minimum energy pathway using a density functional method (BH&H–LYP/6–311G(d,p)) with energies refined at the QCISD(T)/6–311+G(d,p) level, they obtained temperature-dependent TST and improved canonical variational TST (ICVT) rate constants over the range 200–800 K. Arrhenius plots showed reasonable agreement between the calculated and theoretical values of the rate constants at higher temperature; however, the slope was found to be steeper than experiment in both reactions leading to significant discrepancy at lower temperature.

The kinetics of Cl-atom reactions with other classes of heteroatom-containing organic compounds such as HCHO ($k_{298} = 7.3 \times 10^{-11}\,cm^3\,molecule^{-1}\,s^{-1}$) [30] and CH_3SH ($k_{298} = 2.0 \times 10^{-10}\,cm^3\,molecule^{-1}\,s^{-1}$) [30] have received attention, but the rate of reaction of Cl atoms with methylamine remains largely unstudied. Branching between competing channels in these reactions is discussed later.

4.2. *Reaction dynamics*

Inclusion of a functional group or a heteroatom in a molecule of general type CH_3X, where X is not hydrogen or an alkyl group (for convenience, any such molecule will be referred to as being functionalized) enriches the reaction dynamics beyond what is observed for H-atom abstraction from primary, secondary or tertiary carbon sites in alkanes (as discussed in section 2). The functional group may itself contain H atoms, for example in hydroxyl, amino or aldehydic groups, and abstraction from these chemically different environments may display *site-specific dynamics*, which, together with branching ratios for the competing channels, can be explored using selectively deuterated isotopomers.

Interactions between the attacking Cl atom and functionalized molecules are likely to be stronger than found in alkane reactions, leading to the possibility of *entrance-channel effects* directing the dynamics or affecting the product branching ratios. The functionalized radical co-product also possesses properties which can influence the product internal state distributions measured experimentally. Such *exit-channel interactions* are, as will be shown, dominated by dipole–dipole interactions between the polar products.

4.2.1. *Rotational distributions of the HCl products of reactions of Cl atoms with functionalized organic molecules*

Rudić *et al*. reported the first measured nascent HCl rotational distribution of a reaction between Cl atoms and a functionalized organic molecule [160]. Hyperthermal Cl atoms were produced by UV photolysis of molecular chlorine at 355 nm, resulting in a collision energy of 5.6 kcal mol^{-1} for reaction (18) of Cl atoms with methanol, and the nascent HCl ($v' = 0$) products were state-selectively probed using $2+1$ REMPI in a TOF–MS. The reagent gases were expanded into the interaction region using dual pulsed nozzles fitted with narrow-bore tubing to constrain the gas flows. This separation of reagents was necessary to minimize the interaction time before reaction was initiated, lest the reactive signal be overwhelmed by contaminant HCl produced by rapid reaction of the precursors, but was at the expense of substantial cooling in the supersonic expansion. While H-atom abstractions by Cl atoms from alkanes are, so far without exception, found to result in rotationally cold HCl products, as discussed in section 2.2.1, the HCl products of the $Cl + CH_3OH$ reaction show rotational excitation greater than that for thermalized HCl at 298 K. The nascent rotational distributions peak in $J' = 3$ or 4 and are characterized by a temperature of 530 ± 56 K, with a mean rotational energy of $330 \pm 29\,cm^{-1}$. Subsequently, experimental measurements were refined and extended to include the analogous reaction with methanol-d_1 (CH_3OD) and the related reactions with ethanol (reaction 19) and dimethyl ether [152]:

$$Cl + CH_3OCH_3 \rightarrow HCl + CH_3OCH_2 \qquad (21)$$

The HCl ($v' = 0$) rotational distribution observed from reaction with the d_1-deuterated isotopomer of methanol was effectively identical to that of the

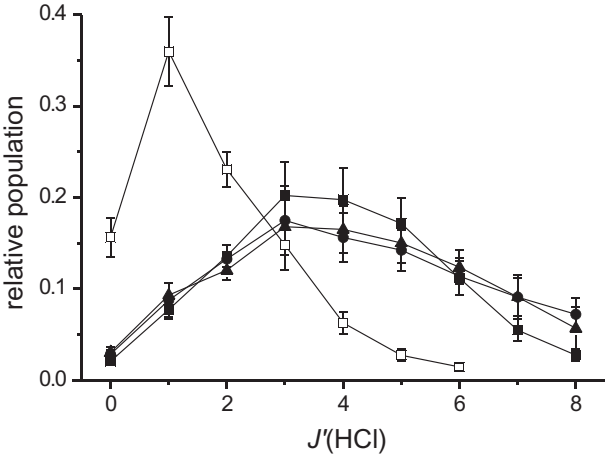

Figure 7. Nascent HCl ($v' = 0$, J') rotational distributions for the reactions of Cl atoms with the oxygenated molecules methanol (▲), ethanol (●), dimethyl ether (■) and, for comparison, ethane (□). Adapted from data originally presented in Ref. [152].

perprotonated reaction, emphasizing the site-specificity of the reaction (abstraction of a methyl H atom) and eliminating the possibility of there being a contribution to the reactive signal of rapid secondary reaction with the hydroxymethyl radical to produce HCl and formaldehyde. Figure 7 highlights both the remarkable similarity of the HCl ($v' = 0$) rotational state distributions observed in these reactions, all of which involve the abstraction of H from a carbon site adjacent to the oxygen heterotaom, and the enhanced rotational excitation relative to that of the $Cl + C_2H_6$ reaction. Comparison with figure 3 demonstrates that the HCl products of reactions (18), (19) and (21) are also much more rotationally excited than those from reactions of Cl atoms with propane and butane (see also Table 2). Recent results from Brouard and co-workers [82], summarized in Table 2, show that abstraction of a secondary H atom from *n*-butane ($\Delta H_{298} = -5.5\,\text{kcal mol}^{-1}$) gives greater rotational excitation than for primary H-atom abstraction ($\Delta H_{298} = -2.0\,\text{kcal mol}^{-1}$), but the mean rotational energy of the HCl of $170\,\text{cm}^{-1}$ in the former case is still much lower than for Cl atom reactions with methanol, ethanol and DME.

Rudić *et al*. argued that the increased product HCl rotational excitation was not simply a consequence of the greater exothermicities of the alcohol and ether reactions compared to that of $Cl + C_2H_6$, since abstraction of a tertiary H atom from isobutane [60] which is comparably exothermic, results in rotationally cold HCl. Consideration of the rotational distributions of the vibrationally excited HCl ($v' = 1$) products observed for $Cl + CH_3CH_2OH$ by Rudić *et al*. [152] and for $Cl + CH_3OH$ by Bechtel *et al*. [161], in a recent revisiting of this reaction using a similar experimental approach, further supports this assertion. For both reactions, despite production of vibrationally excited HCl requiring a significant amount of the available energy, and thus effectively reducing the exothermicity by $\sim 8.5\,\text{kcal mol}^{-1}$, the HCl ($v' = 1$) products also display enhanced rotational excitation, albeit to a lesser degree, and like the HCl ($v' = 0$) products, the distributions are very similar.

The enthalpies of reaction for Cl reactions with monosubstituted halomethanes, (21), are of very similar magnitude to the benchmark $Cl + C_2H_6$ reaction, as shown in Tables 1 and 3. The reactions become less exothermic with increasing size of the halogen substituent, but the total available energy is almost constant for the series

because of the parallel increase in the CM-frame collision energy under typical experimental conditions using Cl atoms from 355-nm photolysis of Cl_2. Murray *et al.* [84] measured the nascent rotational distributions of HCl ($v' = 0$) products of these reactions. The $Cl + CH_3F$ reaction, like the RCH_2OR' (R, R′ = H, CH_3) reactions discussed above, leads to HCl ($v' = 0$) products with much enhanced rotational excitation relative to the benchmark $Cl + C_2H_6$ reaction and the nascent rotational distribution, which peaks in $J' = 3$–4, is most reminiscent of that produced in the more exothermic Cl + DME reaction. For the reactions of the larger methyl halides, the degree of HCl product rotational excitation decreases systematically, although the $Cl + CH_3I$ reaction still forms HCl that is much more rotationally excited than the products of the reaction of $Cl + C_2H_6$. The outcomes of all these measurements are summarized in Table 4. Simple attribution of greater HCl mean rotational energy solely to a larger reaction exothermicity can be discounted although it may be a contributing factor in determining the extent of rotational excitation of HCl. Arguments based on energetics alone also fail to account for the mechanism by which enhanced product rotation is generated because consideration must be given to the source of additional torques. Other factors that may contribute are angular momentum conservation, statistical effects, impulsive energy release from the transition state geometry, the shape of the transition state itself, and post-TS interactions. These possibilities are discussed further below.

In contrast to the reactions of Cl atoms with alcohols, for which abstraction occurs almost exclusively at the α-carbon, the reaction of chlorine with methylamine proceeds competitively via two channels to produce the aminomethyl (CH_2NH_2) and methanaminyl (CH_3NH) radicals:

$$Cl + CH_3NH_2 \rightarrow HCl + CH_2NH_2 \quad (22a)$$

$$\rightarrow HCl + CH_3NH \quad (22b)$$

Using reagents selectively deuterated at the methyl or amine positions, Rudić *et al.* [162] were able to measure site-specific HCl (and DCl) product rotational state distributions and, in conjunction with the observed rotational distributions from the perprotonated and perdeuterated reactions, extract the branching fraction, as shown in figure 8. Despite the aminomethyl channel being more exothermic, and favoured statistically by 3:2, the branching to this channel was found to be only 48% for abstraction of H and 58% for abstraction of D. The branching can be qualitatively explained by consideration of the energies of the *ab initio* stationary points calculated in conjunction with the experimental studies (*vide infra*). The optimized transition states for abstraction at both sites lie lower in energy than the separated reagents and the TS for the less exothermic methanaminyl-producing channel is the lower of the two. The only meaningful 'barrier' to reaction therefore is relative to a pre-reaction molecular complex, which is calculated to be the most stable point on the PES and is formed as a result of a three-centre two-electron bond between the attacking Cl atom and the lone pair on the N atom. Thus, entrance channel interactions between the approaching reagents may play a role in steering the reaction, with the greater density of states for the lower energy methanaminyl-producing transition state channel enhancing the reactivity along that pathway, while the higher energy TS for the more exothermic aminomethyl channel presents a dynamical bottleneck.

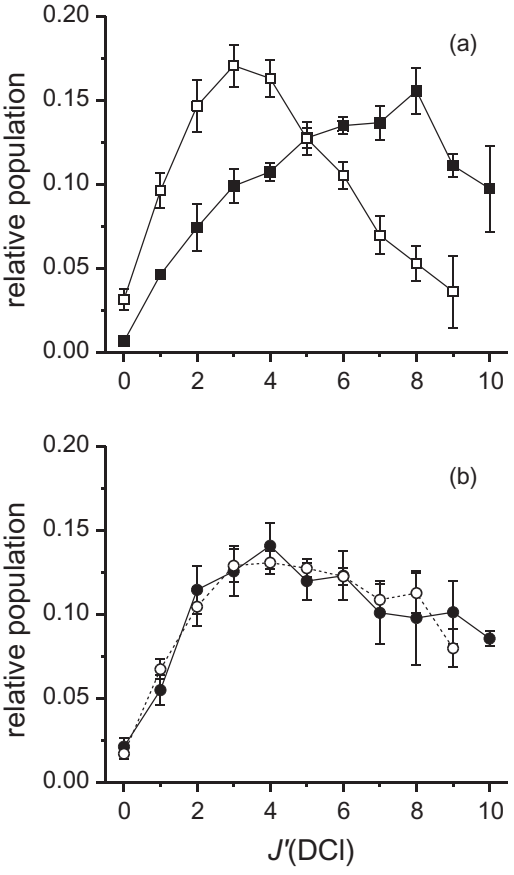

Figure 8. Site-specific (*a*) nascent DCl ($v' = 0$, J') rotational distributions obtained from the reactions of Cl atoms with the selectively deuterated isotopomers methylamine-d_3 (CD_3NH_2) (■) and methylamine-d_2 (CH_3ND_2) (□). The DCl rotational distribution obtained from the reaction of Cl atoms with the perdeuterated isotopomer, methylamine-d_5 (CD_3ND_2) (●) is shown in panel (*b*) along with a best-fit linear combination (○) of the site-specific distributions shown in (*a*). Adapted from data originally presented in Ref. [162].

The rotational distributions observed following reaction at the methyl and amine sites are very different. HCl and DCl molecules produced following reaction at the methyl group were observed to be substantially more rotationally excited than those produced in conjunction with the methanaminyl radical after reaction at the amine site (see Table 4). This observation is surprising because *ab initio* calculations at the MP2/6–311G(d, p) level predict that the C–H–Cl moiety deviates only slightly from collinearity at the transition state, defining an angle of 171.1°, while abstraction at the amine proceeds via a significantly bent transition state with an N–H–Cl angle of 142.0°. Conventional ideas of more bent transition states leading to more rotationally excited products thus clearly do not apply for these H-atom transfer reactions. Standard models of impulsive energy release were found to be unsuitable for reproducing the degree of rotational excitation observed from each channel as they consistently predict more energy (either as a fraction of that available or as an absolute value) to be partitioned into HCl or DCl rotation for the

Table 4. Mean rotational energies, rotational temperatures and rotational fractions of the total available energy for HCl products of reactions of Cl atoms with various functionalized organic molecules at mean collision energies $\langle E_{coll} \rangle$, specified in units of cm^{-1} for ease of comparison with the HCl rotational energies.

Reaction	$\langle E_{coll} \rangle$/ cm^{-1}	$\langle E_{rot} \rangle$/ cm^{-1}	T_{rot} / K	f_{rot}	Reference
$Cl + CH_3OH \rightarrow HCl + CH_2OH$	1960	330 ± 29	530 ± 56	0.071	152
$Cl + CH_3CH_2OH \rightarrow HCl + CH_3CHOH$	2330	340 ± 26	542 ± 38	0.056	152
$Cl + CH_3OCH_3 \rightarrow HCl + CH_2OCH_3$	2330	265 ± 17	418 ± 25	0.057	152
$Cl + CH_3NH_2 \rightarrow HCl + CH_2NH_2$	2000	501 ± 84	720 ± 210	0.091	162
$Cl + CH_3NH_2 \rightarrow HCl + CH_3NH$	2000	122 ± 12	181 ± 16	0.038	162
$Cl + CH_3F \rightarrow HCl + CH_2F$	2030	284 ± 13	403 ± 18	0.092	84
$Cl + CH_3Cl \rightarrow HCl + CH_2Cl$	2410	283 ± 21	380 ± 20	0.087	84
$Cl + CH_3Br \rightarrow HCl + CH_2Br$	3010	226 ± 14	302 ± 12	0.064	84
$Cl + CH_3I \rightarrow HCl + CH_2I$	3290	202 ± 13	291 ± 26	0.065	84

methanaminyl producing channel. Furthermore, impulsive energy release in this reaction would be expected to manifest itself in an isotope effect, with less rotational excitation observed for the DCl products, whereas experimental measurements show near identical mean rotational energies for the HCl and DCl products (501 ± 84 and $508 \pm 17\,cm^{-1}$ for abstraction from a C atom and 122 ± 12 and $157 \pm 12\,cm^{-1}$ for abstraction from an N atom). The conclusion was thus drawn that the PES in the immediate post-transition state region was not strongly repulsive.

Ab initio calculations, performed in conjunction with the experimental measurements of HCl product rotational distributions on the other functionalized reactions [84, 152], predicted near collinear (to within at most $\sim 10^\circ$ of linearity) geometries for the C–H–Cl moiety in the TS in all the systems investigated. Deviation from collinearity is thus unlikely to explain the greater HCl rotation in any of the functionalized systems studied. To illustrate the point, the reactions of Cl atoms with C_2H_6 and CH_3F possess similar thermochemistry and kinematics. *Ab initio* calculations predict a transition state with a C–H–Cl angle of 176.6° for C_2H_6 while the CH_3F reaction proceeds via a saddle point in which the equivalent angle is 177.1°, yet results in significantly more rotationally excited HCl products (see Tables 2 and 4). Indeed, amongst the methyl halide reactions, the transition state bend angle anticorrelates with the degree of rotational excitation measured in the HCl products. Thus, it would appear that such reactions occur largely non-impulsively.

As mentioned in section 4.1, *ab initio* calculations to characterize stationary and saddle points on the PES for the $Cl + CH_3OH$ reaction were performed by Jodkowski *et al.* [147] at the G2 level of theory and used in conjunction with TST to calculate rate constants. These authors also located weakly bound molecular complexes between both reagents and products. For all the functionalized reactive systems discussed the *ab initio* reaction profiles are qualitatively similar, with examples in figure 9, showing a weakly bound pre-reaction complex, as described above for the $Cl + CH_3NH_2$ reaction, in the entrance channel and similarly weakly bound complexes in the products region of the PES [84, 152, 160]. The calculated *ab initio* energy for the $CH_3Br \cdots Cl$ complex is in excellent agreement with the

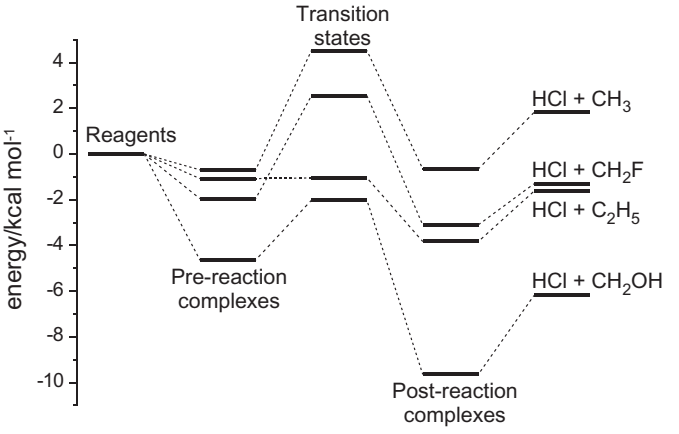

Figure 9. Energies of stationary points (pre- and post-reaction complexes and transition states) calculated at the G2//MP2/6–311G(d,p) level of theory for the reactions of Cl atoms with methane, ethane, methanol and methyl fluoride, as indicated.

experimental value derived from low-temperature kinetic studies of Piety *et al.* [155]. Taatjes and co-workers argued, however, that the considerable fraction of vibrationally excited HCl products, equivalent to the Boltzmann fraction of collisions with sufficient energy to populate HCl ($v' = 1$) under their experimental conditions, was evidence for direct dynamics [149]. Given the shallow nature of the wells and further evidence from scattering experiments discussed later, it seems most probable that these abstraction reactions are indeed direct, or sample only transiently the shallow complexes. Although rotational distributions of HCl have not been calculated using statistical models appropriate for formation of long-lived complexes that account for conservation of energy and total angular momentum, these are unlikely to be applicable because the reactions do not appear to proceed via complexes sufficiently long-lived to randomize the energy among all internal degrees of freedom. The post-TS complexes are computed to be bound by only $\sim 2-3\,\mathrm{kcal\,mol^{-1}}$ with respect to separated products and are thus much more shallow than the potential wells for textbook examples of complex-mechanism reactions of atoms such as $O(^1D)$ [1].

As with Cl-atom reactions with alkanes, angular momentum and kinematic constraints on the dynamics should be weak because both products carry off rotational angular momentum that, for the radical, can be comparable to the orbital angular momentum. This deduction is supported by the very different HCl rotational distributions observed for the kinematically and energetically very similar reactions of Cl atoms with C_2H_6 and CH_3F. The presence of shallow potential wells in the products' region of the PES and the near-linear Cl–H–C moiety in the transition state led Rudić *et al.* [160] to suggest an alternative mechanism to impulsive energy release, statistical considerations, or kinematic constraints, for generating the torque required to produce rotationally excited HCl products.

For the $Cl + RCH_2OR'$ reactions, the post-transition state regions of the PESs were each calculated to support two analogous complexes after abstraction of the α-hydrogen. The first involved an increase in the distance between the C atom and abstracted H atom from the transition state configurations to around 2–3 Å while maintaining collinearity of the $C\cdots H$–Cl moiety. Similar van der Waals complexes

have also been located on the PESs for the reactions of CH_4 and C_2H_6 and were also calculated to be bound by 2–3 kcal mol^{-1}, relative to the products asymptote, and as a result probably play no role in enhancing the nascent HCl rotational excitation [19]. No attempts to locate such structures were made for the reactions of Cl atoms with the methyl halides [84], although an analogous structure was located on the PES for the methylamine reaction [162]. The second class of complex was located in all the functionalized systems described and involves reconfiguration of the molecular geometry such that the nascent HCl is located a similar distance from the radical but with the H atom oriented towards the heteroatom (i.e., a hydrogen bonded type structure). The proposed mechanism for generating rotation is thus that the driving force for this reorientation, associated with an angular anisotropy on the PES, can induce HCl rotation by promoting rapid motion of the H atom with respect to the heavy Cl atom. In essence, the H atom swings around from proximity to the C atom to which it was originally bound, towards the electronegative heteroatom and this motion maps asymptotically into HCl rotation. The mechanism is encouraged by reorientation of the RCHOR′ by rotation induced by the recoil from the reaction TS (with a line of force displaced from the CM of the radical), as is observed in animated trajectories [121]. This proposition is similar in concept to the notion of reorientation of approaching reagents towards a reactive configuration prior to the TS, but is now applied to the separating products.

The reorientation of the nascent HCl products, which ultimately results in enhanced rotational excitation, is thought to be a consequence of the anisotropy of the post-transition state PES which is dominated by dipole–dipole interactions. For the reactions of the methyl halide series, increasing the size of the halogen atom leads to less rotational excitation of the HCl products, in parallel with a reduction of the halomethyl radical dipole moment. In fact, with the exception of the methyl H abstraction in the $Cl + CH_3NH_2$ reaction, which appears to be a special case to be discussed below, there is a direct linear correlation between the average value of $J'(J'+1)$ of the HCl product (proportional to the rotational energy) and the magnitude of the calculated dipole moment of the radical co-fragment. The strength of the correlation is demonstrated in figure 10. It should be stressed that the interaction between HCl and the RCHOR′ (R = H, CH_3) and CH_2X (X = F, Cl, Br, I) is attractive in nature: rotation of the RHCOR′ or CH_2X as the HCl pushes away brings the negatively polarized end of the dipole (located close to the heteroatom) towards the positively polarized H atom in HCl. Rather counter-intuitively, the dipole moment of the aminomethyl fragment is oriented such that the C atom has greater electron density and is the negative end of the radical dipole moment. The rotation of the fragment induced as the products separate thus brings the dipole moments into a more unfavourable alignment with their positive ends pointing towards one another, resulting in a repulsive geared rotational excitation of the HCl. Arguments relating to the interactions of the potential wells and dipole moments in the products' region of the PES can also qualitatively explain the lack of rotation observed following abstraction of an amino H atom. In this case, despite the significantly bent transition state, the system relaxes naturally via the post-reaction complex in which there is a very favourable alignment of the HCl and methanaminyl radical dipole moments, and this serves to counteract any torque that may have been applied to the HCl as the system passes over the transition state region, thus suppressing HCl rotation.

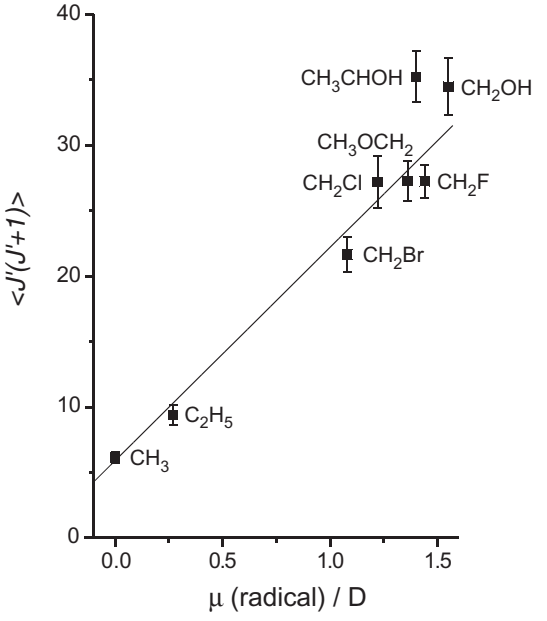

Figure 10. Linear correlation between the mean rotational energy, represented by $\langle J'(J'+1)\rangle$, of nascent HCl products following H-atom abstraction from a carbon site adjacent to a heteroatom, with the *ab initio* dipole moment of the radical co-product calculated at the MP2/6–311G(d,p) level of theory.

Direct dynamics trajectory calculations of the $Cl + CH_4$, C_2H_6 and CH_3OH reactions performed by Rudić *et al.* [19] provide further evidence for the interaction of the products' dipole moments as they separate resulting in enhanced rotational excitation in the latter case. Trajectories were initiated from the transition state using Wigner sampling of the zero-point motion to generate initial conditions. Swarms of trajectories were propagated using *ab initio* electronic structure calculations at the HF/6–31G level to calculate the energies and the forces acting on the atoms at each time step. The resulting calculated HCl rotational distributions were found to overestimate slightly the degree of rotational excitation by one or two quanta, although the overall shapes were in excellent agreement with experimental data. A smaller batch of trajectories propagated using the more accurate MP2/6–311G(d, p) energies and forces for the $Cl + CH_3OH$ reaction was observed to produce a rotational distribution for the HCl products that was in better agreement with experiment, i.e., cooler than the Hartree–Fock level calculations. Dipole moments are overestimated by both HF and MP2 level calculations, and even more so by the former. Animation of representative samples of the trajectories of the $Cl + CH_3OH$ reaction revealed, as described above, that as the products separate, a torque is applied about the CM of the hydroxymethyl product, inducing it to rotate and bringing the electronegative O atom closer to the departing HCl, which is reoriented as a consequence of the trajectory sampling the attractive part of the PES. No such reorientation was observed in the $Cl + CH_4$ or C_2H_6 reactions, despite the presence of shallow potential wells in the products' region of the PESs. The calculations did not, however, suggest that the formation of long-lived complexes played a role, with all the trajectories completing in a time-scale much less than the rotational period of the full system.

Some attention has also been paid to the dynamics of reactions involving aldehydes. Kegley–Owen *et al.* [163] studied the reaction of Cl atoms with acetaldehyde,

$$Cl + CH_3CHO \rightarrow HCl + CH_3CO \quad (23)$$

which proceeds via the exothermic abstraction of the aldehydic H atom, using flash photolysis and tunable diode laser spectroscopy of the HCl products to measure the absolute rate constant directly. The vibrational branching fraction of 0.56 ± 0.15 for production of HCl ($v' = 1$) suggested a slight population inversion and this was later confirmed by a more precise determination of 0.54 ± 0.04 by Smith *et al.* [150] also using tunable diode laser spectroscopy of the HCl products. This significant vibrational excitation of the HCl is consistent with direct abstraction with early release of energy, a conclusion supported by *ab initio* calculations at the MP2/cc–pVDZ level [164] which predicted a very reactant-like, bent transition state. The transition state was calculated to be $0.9\,kcal\,mol^{-1}$ higher in energy than the separated reactants, resulting in a slight barrier to reaction, although correction for the zero-point energy, which would reduce the barrier height, was apparently not considered. Similar calculations were performed to characterize stationary points for the reaction of formaldehyde

$$Cl + HCHO \rightarrow HCl + HCO \quad (24)$$

and again revealed a very early transition state with only a slight barrier to direct abstraction of hydrogen. The calculated barriers are consistent with kinetic data, which suggest no temperature dependence for the $Cl + CH_3CHO$ reaction, albeit over a limited range of 210–340 K, and only a very moderate activation energy of $1\,kcal\,mol^{-1}$ for $Cl + HCHO$, from experimental data over the range 200–500 K. The early barrier and moderate exothermicity of the formaldehyde reaction would suggest vibrational excitation of the HCl products and Seakins *et al.* [150] and Dong *et al.* [165] have observed this experimentally. A population inversion of the HCl products was observed, with the branching fraction for vibrationally excited HCl measured to be 0.91 ± 0.14.

Unlike hydroxyl H atoms, the weak S–H bond in thiols means that abstraction occurs readily. Cheng *et al.* [166] have recently applied time-resolved FTIR spectroscopy to study the reaction of methanethiol, for which the dominant reaction pathway is [167]:

$$Cl + CH_3SH \rightarrow HCl + CH_3S \quad (25)$$

The enthalpy of reaction is similar to abstraction of an aldehydic H atom, and IR chemiluminescent emission was observed for HCl ($v' \leq 3$). Kinetic modelling of the time-dependence of the emission in combination with vibrational surprisal analysis resulted in an inverted vibrational population distribution for HCl ($v' = 0$):($v' = 1$):($v' = 2$):($v' = 3$) of (13 ± 2):(59 ± 2):(22 ± 3):(6 ± 1). Satisfactory fits to the kinetic data required the inclusion of the minor methyl H-atom abstraction pathway. The nascent HCl rotational state distributions for the observed levels were obtained by extrapolating back to zero time and revealed significant rotational excitation for all vibrational levels. This contrasts with the earlier arrested relaxation study of Dill and Heydtmann [168], who reported a bimodal rotational distribution for HCl ($v' = 1$) products, and suggested this was a result of branching between the two product channels. It seems likely that the rotational relaxation in this experiment was

not adequately arrested and that the bimodality was a consequence of slower rotational energy transfer for high-J' products. *Ab initio* calculations performed by Wilson and Hirst [169] and Cheng *et al.* [166] revealed an adduct bound by $\sim$14 kcal mol^{-1} in the entrance channel, analogous to that located for the $Cl + CH_3OH$ reaction, and a reactant-like transition state lying lower in energy than the reagent asymptote. This is consistent with kinetic studies [30] which show a slight negative temperature dependence and no kinetic isotope effect, suggesting adduct formation as the rate-determining step. This deduction is difficult to reconcile, however, with the significant vibrational excitation which suggests a direct abstraction mechanism.

4.2.2. *Scattering dynamics and differential cross-sections*

Steele *et al.* [170] presented the first results of crossed beam scattering experiments on the $Cl + CD_3OD$ reaction at a collision energy of 12.2 kcal mol^{-1} in a neglected paper from 1986. Only products of abstraction of methyl D atoms were observed, despite there being sufficient energy available for reaction at both sites in the molecule, consistent with kinetic studies. The centre-of-mass frame DCl product angular distribution was observed to peak in the forward scattering direction, decreasing gradually to less than half the intensity for back-scattered products, indicating direct scattering dynamics rather than a complex-forming mechanism. There is no other report of dynamical studies of the $Cl + CH_3OH$ reaction in the literature until it was revisited by Suits and co-workers [171, 172] in 2000. These authors also used a crossed molecular beam apparatus to study the reactions of Cl atoms with methanol, ethanol and isopropanol. Velocity map ion images of the organic radical products were recorded following single-photon ionization using the 157 nm output of a F_2 excimer laser. Unwanted ionization of unreacted parent alcohol in the forward scattered region of the ion image resulted in a large background signal in the extreme forward scattering region and measurements in this region were thus deemed unreliable and omitted from the reported angular distributions. The $Cl + CH_3OH$ reaction was studied at a collision energy of 8.7 kcal mol^{-1} and was observed to result in predominantly back-scattered products with a significant sideways component. Contribution of methoxy radicals to the ion signal was discounted, since its ionization potential is greater than the photon energy, allowing unambiguous identification of the products as hydroxymethyl radicals. Despite the noise in the forward-scattered region of the ion images, any possibility of forward scattering was discounted, contrary to the observations of Steele *et al.* [170], and forward–backward symmetry of the angular distribution, and hence a complex forming mechanism, was ruled out. The product velocities were observed to extend almost to the energetic limit, although the peak in the kinetic energy distribution was lower, indicating internal (rotational or vibrational) excitation of the hydroxymethyl radical, with 39% on average of the available energy partitioned into translation.

For the ethanol and isopropanol reactions, arguments based on the radical ionization potentials and evidence from kinetic studies described above, led to the radical products being identified as the 1-hydroxyethyl and 1-hydroxy-1-methylethyl radicals, respectively, following the thermodynamically favoured α-hydrogen abstraction pathways. The reaction involving ethanol was investigated at collision energies of 6.0 and 9.7 kcal mol^{-1}, and the angular scattering distribution was again found to peak in the backward direction, with the sideways-scattered component

observed to increase at the higher collision energy, although the total translational energy release was near constant at 32–38%. The greater side scatter was interpreted as a consequence of larger impact parameter collisions playing a greater role, also leading to greater radical internal excitation. Sideways-scattering collisions couple the available energy into the radical internal modes more effectively, as evidenced by the greater average translational energy for the back-scattered products at the lower collision energy. The reaction of isopropanol at a collision energy of 11.9 kcal mol^{-1} also resulted in predominantly back-scattered products (although it must be remembered that the experiments were blind to the forward-scattering region) and a similar partitioning of the available energy, with 31% going to translational motion.

An alternative approach, employing velocity map ion imaging to study chemical reactions with product quantum state resolution, has been pioneered by Toomes and Kitsopoulos [81]. Unskimmed beams of molecular chlorine and the organic molecular co-reagent are expanded from parallel pulsed nozzles, offset vertically. By taking advantage of the almost purely perpendicular ($\beta = -1$) photodissociation of Cl_2 at 355 nm, a beam of Cl atoms is generated which intersects the organic co-reagent molecular beam at right angles and the products scatter into the probe laser focal volume, where they are ionized via a 2 + 1 REMPI process and accelerated towards a position-sensitive detector by electric fields configured for velocity mapping. Murray *et al.* [173] applied this technique to measure the state-resolved differential cross-sections of the reactions of Cl atoms with methanol and dimethyl ether leading to HCl products in $v' = 0$, covering the most populated rotational states $J' = 2$–5, as determined from previous measurements at the same collision energy [152]. Representative data are shown in figure 11. The differential cross-sections extracted from the images for the $Cl + CH_3OH$ reactions show broad angular distributions with intensity peaking in the forward and backward hemispheres, and are almost independent of J'. A more marked J' dependence in the angular distributions was observed for the HCl products of the $Cl + CH_3OCH_3$ reaction, which peaked in the forward direction for low-J' and became increasingly back-scattered at higher J', showing a qualitative similarity to the $Cl + C_2H_6$ and n-C_4H_{10} reactions. Such results can be understood in terms of arguments used for the alkane reactions, with lower impact parameter collisions leading to greater backward scatter and the associated more repulsive interaction inducing HCl rotation. The kinetic energy release, integrated over all scattering angles, in both reactions studied was very similar, and in excellent agreement with the results of Ahmed *et al.* [171, 172] showing, on average, around 40% of the available energy deposited into product translation. Sideways-scattered products exhibit a smaller kinetic energy release than those back-scattered, consistent with the VUV ionization experiments [171, 172]. The forward/backward scattering might be attributed to a long-lived complex, but the shallow wells on the PES suggest an alternative mechanism involving direct dynamics at a range of impact parameters.

The centre-of-mass angular scattering distributions for HCl ($v' = 1$) products of the $Cl + CH_3OH$ reaction derived from core-extracted time-of-flight profiles have been reported by Bechtel *et al.* [161]. The measured speed distributions were unchanged for $J' = 1$, 3 and 5 products and displayed a steady increase up to the maximum allowed speed, while analysis of the spatial anisotropy of the profiles led to the conclusion that very little energy was partitioned into internal modes of the hydroxymethyl radical. In contrast, the analogous measurements of the HCl

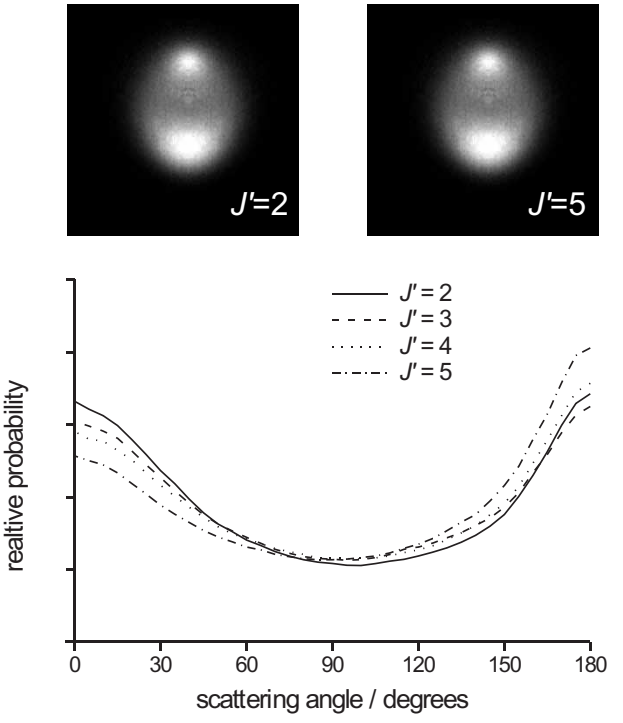

Figure 11. Representative ion images of the nascent HCl ($v'=0$, J') products formed with $J'=2$ and $J'=5$ from the reaction of Cl atoms with methanol, and corresponding angular distributions for the $J'=2$–5 products derived from direct integration of the images. Vertically downward in the images corresponds to forward scattering of products in the centre-of-mass frame. Adapted from data originally presented in Ref. [173].

($v'=0$) products resulted in speed distributions, again independent of J', which peaked below the maximum allowed and suggested significant radical excitation, consistent with the ion-imaging data [171–173]. Transformation of the HCl ($v'=1$) speed distributions gave CM frame angular distributions with maximum intensity in the forward-scattered region, which was interpreted as being due to a stripping mechanism with reaction occurring at large impact parameters and the radical co-product effectively acting as a spectator. The radical internal excitation precluded extraction of the angular distribution for the HCl ($v'=0$) products using this technique, but the observations for $v'=1$ are again consistent with the notion of the near-thermoneutral channel being associated with large-b, peripheral collisions with no deflection of the forward trajectory because there is little or no repulsive energy release [95].

Recently, Toomes *et al.* [174] studied the reactions of Cl atoms with CH_3Cl and CH_3Br using the same velocity map imaging method as was employed for $Cl + CH_3OH$ and DME reactions. Images were recorded for the same $J'=2$–5 rotational levels of the $v'=0$ HCl products. From the resulting images, the reactive scattering of the methyl halide reactions could immediately be seen to be different from that of the $Cl + CH_3OH$ and CH_3OCH_3 reactions. Maximum intensity was observed in the back-scattered region and the angular distributions were effectively independent of the HCl product angular momentum. The preference for back-

scattering was more pronounced in the $Cl + CH_3Cl$ reaction than $Cl + CH_3Br$, for which the angular distribution was almost isotropic. Kinetic energy release distributions derived from the images showed approximately 24% of the available energy partitioned into product translation for both of the methyl halide reactions studied, which is notably less than the $Cl + CH_3OR$ ($R = H$, CH_3) reactions. Rotational excitation of the HCl products accounted for only a small fraction of the available energy, indicating that internal excitation of the halomethyl co-products was substantially greater.

While the nascent HCl rotational excitation in the reactions of Cl atoms with functionalized organic molecules is plausibly a result of long-range anisotropic dipole–dipole interactions in the exit channel, the angular scattering is determined by shorter-range interactions. This is demonstrated by the similarity of the nascent HCl ($v' = 0$) rotational distributions observed for the reactions of Cl atoms with methanol and dimethyl ether and the disparity in the observed angular scattering. The angular distributions can be explained, qualitatively at least, by consideration of the PES in the transition state region, with reference to the more established understanding of the dynamics of the benchmark reactions of methane and ethane. The reactions which lead to predominantly back-scattered products, namely $Cl + CH_4$, CH_3Cl and, to a lesser extent, CH_3Br, are also those which proceed over a barrier. *Ab initio* calculations to characterize the transition states [84, 174] predict an essentially collinear geometry in all cases and, more importantly, relatively high-frequency transverse bending modes, indicating a steeply rising potential for any non-collinear Cl-atom approach. Coupled with the barrier to reaction, this constrains reactive encounters to small impact parameter collisions, favouring back-scattered products. For $Cl + CH_4$, the C_{3v} symmetry of the transition state results in two degenerate orthogonal high-frequency bending modes. Substituting an H atom with a halogen atom reduces the symmetry of the transition states to C_s and causes a decrease in the frequency, and consequently a relaxation of the potential, of bending vibrations in the symmetry plane. This effectively relaxes the constraint on collinearity, leading to more side- and forward-scattered products.

The reactions of Cl atoms with C_2H_6 and CH_3OR' ($R = H$, CH_3) lead to far broader angular scattering of the nascent HCl products. *Ab initio* calculations [152] predict these H-atom abstraction reactions to be barrierless, with respect to the reagents, and in contrast to the $Cl + CH_3X$ ($X = H$, Cl, Br) reactions described above, the transition states are characterized by low-frequency bending vibrations. Hence, the energetic penalty for non-collinear attack of the Cl atom is smaller, allowing abstraction to occur via a wide range of impact parameters including large-b collisions that result in more forward scattering of the products. The very subtle J'-dependence of the products of the reactions of the oxygenated molecules is in contrast to the $Cl + C_2H_6$ reaction, which was observed to result in increased back-scatter for higher J' HCl products as a result of more impulsive, small impact parameter encounters, while forward-scattered products possessed less rotational excitation as a result of non-impulsive H-atom transfer during a glancing collision. We have previously suggested that the exit channel dipole–dipole interactions for $Cl + CH_3OH$, which are effectively absent for the $Cl + C_2H_6$ reaction, served to mix the J' values of the HCl long after the scattering angles have been determined by short-range forces. Similar arguments can be applied to account for the absence of any J'-dependence of the scattering of the HCl products of the methyl halide reactions.

5. Summary and conclusions

The preceding sections have reviewed the current state of knowledge of the kinetics, thermochemistry and dynamics of reactions of Cl atoms with a variety of organic molecules in which an H atom is abstracted. For functionalized molecules such as methanol, ethanol, dimethyl ether, and the methyl halides, the H atom is removed from a carbon atom bonded to the heteroatom in the functional group, and in all these cases the HCl is observed to be much more rotationally excited than the products of reactions of Cl atoms either with straight-chain, branched or cyclic saturated hydrocarbons (see Tables 2 and 4). The extent of rotational excitation of the HCl does not correlate with the bend angle away from linearity of the Cl–H–C moiety in the transition state for reaction, as might be expected for impulsive transfer of H between the two heavier atoms. Indeed, calculations suggest minimum energy structures for all the transition states in which the Cl–H–C angle deviates by only a few degrees from collinear. Although reactions will not necessarily proceed through this minimum energy geometry, it will reflect the likely preferred geometries for reaction. The bending motion of the H atom within the transition state could also map onto asymptotic HCl rotation, but no correlation is found between the computed bending frequencies and the mean rotational energy of the HCl. Reaction exothermicity might be expected to determine the rotational excitation of products, but again no clear-cut correlation is identified, although there is a trend within the alkane systems for more exothermic channels to form HCl with more rotational energy. More influential might be the energetic height of the TS above the products, and whether the TS is located early or late along the reaction coordinate, with both affecting the extent of impulsive energy release, but the available evidence is not yet compelling.

We have therefore presented arguments for an additional source of HCl rotation arising from dipole–dipole interactions associated with the post-TS region of the PES as the products separate. This mechanism acts only weakly for the reactions of Cl atoms with alkanes because the alkyl radical products have very small dipole moments, but appears to be important for reaction with functionalized organic molecules. A clear correlation has been demonstrated between the mean rotational energy of the HCl and the dipole moment of the radical co-product. *Ab initio* calculations identify the presence of shallow wells on this part of the PES that are associated with an attractive interaction between the HCl and the polar radical. These wells, or the angular anisotropy of the product valley of the PES, may reorient the internuclear axes of the products towards a more energetically favourable configuration involving a hydrogen bonded type structure. Trajectory calculations clearly illustrate this type of dynamical behaviour, and show that transfer of the H atom from carbon to chlorine forces the radical product to rotate in such a way as to bring the negatively polarized heteroatom towards the positive end of the dipole in HCl, thereby inducing HCl rotation. New experimental methods involving uptake of radicals at very low temperatures within helium nanodroplets may be able to characterize spectroscopically the structures of these post-TS complexes [175]. We cannot fully discount the possibility of trapping within these wells, or scattering from them resulting in some statistical redistribution of energy among the vibrational and rotational modes of the products, but the wells are shallow and no such effects are observed for the reactions of Cl with alkanes, which exhibit similar post-TS potential energy minima (but lack the dipole–dipole induced anisotropy). If our interpretation of the dynamics is correct, it highlights the importance of the shape,

structure and polarity of the polyatomic radical co-product in influencing the reaction dynamics. Traditional quasi-classical trajectory calculations in reduced dimensionality have proved very successful in the study of the reaction of Cl atoms with methane [43], with the methyl group treated as a single particle. Such a pseudo-triatomic approach is unlikely to be so successful, however, for the other reactions considered in this review, because the radical products formed together with the HCl, such as ethyl, hydroxymethyl and CH_2X, absorb significant fractions of the available energy in their rotational and vibrational modes as well as interacting with the HCl via long-range dipolar forces. Direct dynamics trajectories computed on-the-fly in full dimensionality offer a promising alternative to these QCT methods [19].

The proposed mechanism for rotational excitation of HCl requires the time-scale for reorientation of the dipoles of the radical product and the HCl to be sufficiently fast to occur before the products have separated to a distance over which the dipolar interactions are too weak to be of consequence. In this regard, the reactions of Cl atoms are very favourable because they are not especially exothermic, so translational energy release is limited, and the heavy HCl recoils only slowly from the radical. With the aid of on-the-fly trajectory calculations, we are currently exploring the effect of greater translational energy in the products, and thus a shorter interaction time before separation.

In contrast to the rotational distributions of the HCl products of the various reactions, the scattering dynamics of Cl atoms with alkanes and with functionalized molecules are broadly similar and can both be qualitatively understood by using simple arguments based on the range of impact parameters that can lead to products. Those reactions with negligible barriers (e.g., $Cl + C_2H_6$ and $Cl + CH_3OH$) show broad angular distributions of products in the differential cross-section because reaction can occur right out to trajectories in which the Cl atom attacks at the periphery of the molecule. In contrast, reactions of Cl atoms with methane and the methyl halides have small but significant barriers that inhibit reaction at large impact parameters and favour backward and sideways scattered products arising from lower-b collisions. Evidence from reactions of Cl atoms with ethane and butane suggests that the more backward-scattered HCl products have higher rotational excitation because of greater impulsive energy release than for the glancing collisions that lead to forward scatter. For reaction of Cl atoms with methanol and the methyl halides, however, such correlations between J' and scattering angle are largely washed out, and we propose that this is a consequence of the long-range dipolar interactions affecting the HCl rotational motion as the newly formed products separate.

Work is in progress to examine the effect of structure of the organic molecule on the reaction dynamics. Towards this objective, we have examined the HCl products of reaction of Cl atoms with the highly constrained cyclic organic molecules oxirane (c-C_2H_4O) and thiirane (c-C_2H_4S), and hope to distinguish any dynamics of ring-retaining versus ring-opening mechanisms following abstraction of an H atom. Future prospects also include attempts to control the branching of reactions such as $Cl + CH_3OH$ or $Cl + CH_3NH_2$ in which there is the possibility of abstraction of an H atom either from a methyl or a hydroxyl or amino group. One approach might be to excite vibrational local modes of these molecules to promote reaction at one site.

Considerable strides have been taken in recent years to understand the model systems of reactions of H, F, O and Cl atoms with a range of polyatomic molecules.

Future efforts will inevitably focus on replacing the atomic reagent by a radical such as OH, CN or CH_3, necessitating development of new experimental and theoretical methods capable of delivering quantum-state specific scattering data. Exploration of the dynamics of reactions of atoms and radicals in condensed phases such as *liquid* organic compounds also presents new and stimulating challenges.

Acknowledgements

We are very grateful to Svemir Rudić, Jeremy N. Harvey, Julie K. Pearce, Bertrand Retail, Paul N. Stevens and Keith N. Rosser for their contributions to the work carried out at the University of Bristol. Imaging experiments were carried out in collaboration with Theofanis N. Kitsopoulos, Rachel L. Toomes and Alrik J. van den Brom at the Ultraviolet Laser Facility operating at FORTH, Crete (with financial support from HP, Access to Large Scale Facilities EU program, contract No. HPRN–CT–1999–00007 and EU Research and Training Networks *PICNIC* HPRN–CT–2002–00183 and *REACTIVES* HPRN–CT–2000–0006). Financial support for the Bristol group from the EPSRC Portfolio Grant *LASER* is gratefully acknowledged. We thank M. Brouard and D. J. Nesbitt for valuable discussions and for provision of unpublished results, and K. Liu for providing figure 4.

References

[1] R. D. Levine, and R.B. Bernstein, Molecular Reaction Dynamics and Chemical Reactivity (New York: Oxford University Press) (1987).
[2] J. M. Bowman, and G. C. Schatz, Ann. Rev. Phys. Chem. **46**, 169 (1995).
[3] S. C. Althorpe, and D. C. Clary, Ann. Rev. Phys. Chem. **54**, 493 (2003).
[4] F. Ausfelder, A. E. Pomerantz, R. N. Zare, S. C. Althorpe, F. J. Aoiz, L. Banares, and J. F. Castillo, J. Chem. Phys. **120**, 3255 (2004).
[5] M. H. Alexander, D. E. Manolopoulos, and H.-J. Werner, J. Chem. Phys. **113**, 11084 (2000).
[6] M. H. Alexander, G. Capecchi, and H.-J. Werner, Science. **296**, 715 (2002).
[7] F. Fernández-Alonso, and R. N. Zare, Ann. Rev. Phys. Chem. **53**, 67 (2002).
[8] K. Liu, R. T. Skodje, and D. E. Manolopoulos, Phys. Chem. Comm. **5**, 27 (2002).
[9] R. T. Skodje, D. Skouteris, D. E. Manolopoulos, S.-H. Lee, F. Dong, and K. Liu, J. Chem. Phys. **112**, 4536 (2000).
[10] R. T. Skodje, D. Skouteris, D. E. Manolopoulos, S.-H. Lee, F. Dong, and K. Liu, Phys. Rev. Lett. **85**, 1206 (2000).
[11] M. J. Pilling, and P. W. Seakins, Reaction Kinetics (Oxford: Oxford University Press) (1996).
[12] R. P. Wayne, Chemistry of Atmospheres, 3rd edition (Oxford: Oxford University Press) (2000).
[13] M. Garcia-Viloca, J. Gao, M. Karplus, and D. G. Truhlar, Science. **303**, 186 (2004).
[14] T. Brixner, and G. Gerber, Chem. Phys. Chem. **4**, 418 (2003).
[15] F. F. Crim, Acc. Chem. Res. **32**, 877 (1999).
[16] D. J. Nesbitt, and R. W. Field, J. Phys. Chem. **100**, 12735 (1996).
[17] X. Wang, M. Ben-Nun, and R. D. Levine, Chem. Phys. **197**, 1 (1995).
[18] M. A. Collins, Theo. Chem. Accounts. **108**, 313 (2002).
[19] S. Rudić, C. Murray, J. N. Harvey, and A. J. Orr-Ewing, J. Chem. Phys. **120**, 186 (2004).
[20] F. Ausfelder, and K. G. McKendrick, Prog. React. Kinet. Mech. **25**, 299 (2000).
[21] M. J. Bronikowski, W. R. Simpson, B. Girard, and R. N. Zare, J. Chem. Phys. **95**, 8647 (1991).
[22] M. J. Bronikowski, W. R. Simpson, and R. N. Zare, J. Phys. Chem. **97**, 2194 (1993).
[23] M. J. Bronikowski, W. R. Simpson, and R. N. Zare, J. Phys. Chem. **97**, 2204 (1993).

[24] J. P. Camden, H. A. Bechtel, and R. N. Zare, Angew. Chem. Int. Ed. **42**, 5227 (2003).
[25] N. S. Shuman, A. Srivastava, C. A. Picconatto, D. S. Danese, P. C. Ray, and J. J. Valentini, J. Phys. Chem. A. **107**, 8380 (2003).
[26] S. R. Langford, P. M. Regan, A. J. Orr-Ewing, and M. N. R. Ashfold, Chem. Phys. **231**, 245 (1998).
[27] P. M. Regan, S. R. Langford, A. J. Orr-Ewing, and M. N. R. Ashfold, J. Chem. Phys. **110**, 281 (1999).
[28] R. Atkinson, D. L. Baulch, R. A. Cox, R. F. Hampson Jr, J. A. Kerr, and J. Troe, J. Phys. Chem. Ref. Data. **21**, 1125 (1992).
[29] R. Atkinson, D. L. Baulch, R. A. Cox, R.F. Hampson Jr, J. A. Kerr, M. J. Rossi, and J. Troe, J. Phys. Chem. Ref. Data. **28**, 191 (1999).
[30] R. Atkinson, D. L. Baulch, R. A. Cox, J. N. Crowley, R.F. Hampson Jr, J. A. Kerr, M. J. Rossi, and J. Troe, Summary of evaluated kinetic and photochemical data for atmospheric chemistry. Web version: http://www.iupac-kinetic.ch.cam.ac.uk/ (2003).
[31] B. J. Finlayson-Pitts, Chem. Rev. **103**, 4801 (2003).
[32] J. D. DeSain, S. J. Klippenstein, C. A. Taatjes, M. D. Hurley, and T. J. Wallington, J. Phys. Chem. A. **107**, 1992 (2003).
[33] NIST Atomic Spectra Database (http://physics.nist.gov/cgi-bin/AtData/main_asd).
[34] A. R. Ravishankara, and P. H. Wine, J. Chem. Phys. **72**, 25 (1980).
[35] H. A. Michelsen, and W. R. Simpson, J. Phys. Chem. A. **105**, 1476 (2001).
[36] N. M. Donahue, J. S. Clarke, and J. G. Anderson, J. Phys. Chem. A. **102**, 3923 (1998).
[37] T. N. Truong, D. G. Truhlar, K. K. Baldridge, M. S. Gordon, and R. Steckler, J. Chem. Phys. **90**, 7137 (1989).
[38] K. D. Dobbs, and D. A. Dixon, J. Phys. Chem. **98**, 12584 (1994).
[39] J. C. Corchado, D. G. Truhlar, and J. Espinosa-García. J. Chem. Phys. **112**, 9375 (2000).
[40] J. Espinosa-García, and J. C. Corchado, J. Chem. Phys. **105**, 3517 (1996).
[41] E. Garcia, C. Sánchez, A. Saracibar, and A. Laganà, J. Phys. Chem. A. **108**, 8752 (2004).
[42] W. T. Duncan, and T. N. Truong, J. Chem. Phys. **103**, 9642 (1995).
[43] D. Troya, J. Millán, I. Banos, and M. González, J. Phys. Chem. **117**, 5730 (2002).
[44] W. T. Duncan, and T. N. Truong, erratum, J. Chem. Phys. **109**, 3703 (1998).
[45] J. S. Pilgrim, A. McIlroy, and C. A. Taatjes, J. Phys. Chem. A. **101**, 1873 (1997).
[46] D. Sarzynski, and B. Sztuba, Int. J. Chem. Kinet. **34**, 651 (2002).
[47] P. Cadman, A. W. Kirk, and A. F. Trotman-Dickenson, J. Chem. Soc. Chem. Commun. **72**, 1027 (1976).
[48] P. A. Hooshiyar, and H. Niki, Int. J. Chem. Kinet. **27**, 1197 (1995).
[49] M. H. Baghal-Vayjooee, and S. W. Benson, J. Am. Chem. Soc. **101**, 2838 (1979).
[50] M. D. Hurley, W. F. Schneider, T. J. Wallington, D. J. Mann, J. D. DeSain, and C. A. Taatjes, J. Phys. Chem. A. **107**, 2003 (2003).
[51] A. Bottoni, and G. Poggi, J. Molec. Structure (Theochem), **337**, 161 (1995).
[52] O. Roberto-Neto, and F. B. C. Machado, Theor. Chem. Acc. **107**, 15 (2001).
[53] O. Roberto-Neto, and F. B. C. Machado, J. Molec. Struct. Theo. Chem. **580**, 161 (2002).
[54] J. S. Pilgrim, and C. A. Taatjes, J. Phys. Chem. A. **101**, 5776 (1997).
[55] J. S. Pilgrim, and C. A. Taatjes, J. Phys. Chem. A. **101**, 4172 (1997).
[56] J. T. Farrell, and C. A. Taatjes, J. Phys. Chem. A. **102**, 4846 (1998).
[57] K. C. Kim, and D. W. Setser, J. Phys. Chem. **77**, 2493 (1973).
[58] Y.-F. Yen, Z. Wang, B. Xue, and B. Koplitz, J. Phys. Chem. **98**, 4 (1994).
[59] D. F. Varley, and P. J. Dagdigian, Chem. Phys. Lett. **255**, 393 (1996).
[60] D. F. Varley, and P. J. Dagdigian, J. Phys. Chem. **100**, 4365 (1996).
[61] J. Park, Y. Lee, J. F. Hershberger, J. M. Hossenlopp, and G. W. Flynn, J. Am. Chem. Soc. **114**, 58 (1992).
[62] X. Liu, R. L. Gross, G. E. Hall, J. T. Muckerman, and A. G. Suits, J. Chem. Phys. **117**, 7947 (2002).
[63] P. Andresen, and A. C. Luntz, J. Chem. Phys. **72**, 5842 (1980).
[64] A. C. Luntz, and P. Andresen, J. Chem. Phys. **72**, 5851 (1980).
[65] W. R. Simpson, A. J. Orr-Ewing, and R. N. Zare, Chem. Phys. Lett. **212**, 163 (1993).

[66] W. R. Simpson, A. J. Orr-Ewing, and R. N. Zare, SPIE Proceedings. **1858**, 476 (1993).
[67] W. R. Simpson, A. J. Orr-Ewing, T. P. Rakitzis, S. A. Kandel, and R. N. Zare, J. Chem. Phys. **103**, 7299 (1995).
[68] W. R. Simpson, T. P. Rakitzis, S. A. Kandel, A. J. Orr-Ewing, and R. N. Zare, J. Chem. Phys. **103**, 7313 (1995).
[69] W. R. Simpson, T. P. Rakitzis, S. A. Kandel, T. Lev-On, and R. N. Zare, J. Phys. Chem. **100**, 7938 (1996).
[70] S. A. Kandel, T. P. Rakitzis, T. Lev-On, and R. N. Zare, J. Chem. Phys. **105**, 7550 (1996).
[71] S. A. Kandel, T. P. Rakitzis, T. Lev-On, and R. N. Zare, Chem. Phys. Lett. **265**, 121 (1997).
[72] T. P. Rakitzis, S. A. Kandel, T. Lev-On, and R. N. Zare, J. Chem. Phys. **107**, 9392 (1997).
[73] S. A. Kandel, T. P. Rakitzis, T. Lev-On, and R. N. Zare, J. Phys. Chem. A. **102**, 2270 (1998).
[74] S. A. Kandel, and R. N. Zare, J. Chem. Phys. **109**, 9719 (1998).
[75] N. E. Shafer, A. J. Orr-Ewing, W. R. Simpson, H. Xu., and R. N. Zare, Chem. Phys. Lett. **212**, 155 (1993).
[76] F. J. Aoiz, M. Brouard, P. A. Enriquez, and R. Sayos, J. Chem. Soc. Faraday Trans, **89**, 1427 (1993).
[77] M. Ben-Nun, M. Brouard, J. P. Simons, and R. D. Levine, Chem. Phys. Lett. **210**, 423 (1993).
[78] M. J. Bass, M. Brouard, C. Vallance, T. N. Kitsopoulos, P. C. Samartzis, and R. L. Toomes, J. Chem. Phys. **119**, 7168 (2003).
[79] D. A. Blank, N. Hemmi, A. G. Suits, and Y. T. Lee, Chem. Phys. **231**, 261 (1998).
[80] D. F. Varley, and P. J. Dagdigian, J. Phys. Chem. **99**, 9843 (1995).
[81] R. L. Toomes, and T. N. Kitsopoulos, Phys. Chem. Chem. Phys. **5**, 2481 (2003).
[82] M. J. Bass, M. Brouard, C. Vallance, T. N. Kitsopoulos, P. C. Samartzis, R. L. Toomes, J. Chem. Phys. **121**, 7175 (2004).
[83] N. Hemmi, and A. G. Suits, J. Chem. Phys. **109**, 5338 (1998).
[84] C. Murray, B. Retail, and A. J. Orr-Ewing, Chem. Phys. **301**, 239 (2004).
[85] H. Tsurumaki, Y. Fujimura, and O. Kajimoto, J. Chem. Phys. **112**, 8338 (2000).
[86] K. E. Holdy, L. C. Klotz, and K. R. Wilson, J. Chem. Phys. **52**, 4588 (1970).
[87] G. E. Busch, and K. R. Wilson, J. Chem. Phys **56**, 3626 (1972).
[88] D. S. Moore, D. S. Bomse, and J. J. Valentini, J. Chem. Phys. **79**, 1745 (1983).
[89] H. B. Levene, and J. J. Valentini, J. Chem. Phys. **87**, 2594 (1987).
[90] P. M. Aker, G. J. Germann, and J. J. Valentini, J. Chem. Phys. **90**, 4795 (1989).
[91] A. J. McCaffery, Phys. Chem. Chem. Phys. **6**, 1637 (2004).
[92] C. A. Picconatto, Srivastava, and J. J. Valentini, J. Chem. Phys. **114**, 1663 (2001).
[93] C. Vallance, and M. Brouard, private communication (2004).
[94] J. Zhou, J. J. Lin, B. Zhang, and K. Liu, J. Phys. Chem. A. **108**, 7832 (2004).
[95] Z. H. Kim, H. A. Bechtel, and R. N. Zare, J. Chem. Phys. **117**, 3232 (2002).
[96] A. J. Orr-Ewing, J. Chem. Soc. Faraday Trans. **92**, 881 (1996).
[97] A. J. Orr-Ewing, and R. N. Zare, Ann. Rev. Phys. Chem. **45**, 315 (1994).
[98] T. P. Rakitzis, S. A. Kandel, T. Lev-On, and R. N. Zare, J. Chem. Phys. **107**, 9392 (1997).
[99] L. Zhang, M.-D. Chen, M.-L. Wang, and K.-L. Han, J. Chem. Phys. **112**, 3710 (2000).
[100] A. J. Orr-Ewing, W. R. Simpson, T. P. Rakitzis, S. A. Kandel, and R. N. Zare, J. Chem. Phys. **106**, 5961 (1997).
[101] M.-D. Chen, M.-L. Wang, K.-L. Han, and S.-L. Ding, Chem. Phys. Lett. **301**, 303 (1999).
[102] A. G. Suits, Modern Trends in Chemical Reaction Dynamics Part 1: Experiment and Theory, edited by X. Yang and K. Liu (Singapore: World Scientific) (2004).
[103] S. Yoon, S. Henton, A. N. Zivkovic, and F. F. Crim, J. Chem. Phys. **116**, 10744 (2002).
[104] J. R. Fair, D. Schaefer, R. Kosloff, and D. J. Nesbitt, J. Chem. Phys. **116**, 1406 (2002).
[105] L. Halonen, S. L. Bernasek, and D. J. Nesbitt, J. Chem. Phys, **115**, 5611 (2001).

[106] S. Yoon, R. J. Holiday, E. L. Sibert, and F. F. Crim, J. Chem. Phys. **119**, 9568 (2003).
[107] H. A. Bechtel, J. P. Camden, D. J. Ankeny Brown, and R. N. Zare, J. Chem. Phys. **120**, 5096 (2004).
[108] Z. H. Kim, H. A. Bechtel, and R. N. Zare, J. Am. Chem. Soc. **123**, 12714 (2001).
[109] H. A. Bechtel, Z. H. Kim, J. P. Camden, and R. N. Zare, J. Chem. Phys. **120**, 791 (2004).
[110] S. Yoon, R. J. Holiday, and F. F. Crim, J. Chem. Phys. **119**, 4755 (2003).
[111] Y.-J. Chen, L.-K. Chu, S.-R. Lin, and Y.-P. Lee, J. Chem. Phys. **115**, 6513 (2001).
[112] F. Dong, S. H. Lee, and K. Liu, J. Chem. Phys. **115**, 1197 (2001).
[113] D. M. Neumark, A. M. Wodtke, G. N. Robinson, C. C. Hayden, and Y. T. Lee, J. Chem. Phys. **82**, 3045 (1985).
[114] S. A. Nizkorodov, W.A. Harper, and D. J. Nesbitt, Faraday Discuss. **113**, 107 (1999).
[115] S. A. Nizkorodov, W. A. Harper, W. B. Chapman, B. W. Blackmon, and D. J. Nesbitt, J. Chem. Phys. **111**, 8404 (1999).
[116] Y.-R. Tzeng, and M. H. Alexander, J. Chem. Phys. **121**, 5812 (2004).
[117] Z. H. Kim, A. J. Alexander, H. A. Bechtel, and R. N. Zare, J. Chem. Phys. **115**, 179 (2001).
[118] Y. Matsumi, K. Izumi, V. Skorokhodov, M. Kawasaki, and N. Tanaka, J. Phys. Chem. A. **101**, 1216 (1997).
[119] K. Hitsuda, K. Takahashi, Y. Matsumi, and T. J. Wallington, Chem. Phys. Lett. **346**, 16 (2001).
[120] A. Fernández-Ramos, E. Martínez-Núnez, J. M. C. Marques, and S. A. Vázquez, J. Chem. Phys. **118**, 6280 (2003).
[121] http://www.chm.bris.ac.uk/pt/ajoe/trajectories/
[122] G. Nyman, H.-G. Yu, and R. B. Walker, J. Chem. Phys. **109**, 5896 (1998).
[123] H.-G. Yu, and G. Nyman, Phys. Chem. Chem. Phys. **1**, 1181 (1999).
[124] H.-G. Yu, and G. Nyman, J. Chem. Phys **111**, 6693 (1999).
[125] H.-G. Yu, and G. Nyman, J. Chem. Phys. **110**, 7233 (1999).
[126] S. Sokov, and J. M. Bowman, J. Chem. Phys. **113**, 4495 (2000).
[127] D. Troya, J. Millán, I. Banos, and M. González, J. Chem. Phys. **120**, 5181 (2004).
[128] J. C. Corchado, and J. Espinosa-García, J. Chem. Phys. **105**, 3152 (1996).
[129] J. Zhou, J. J. Lin, W. Shiu, S.-C. Pu, and K. Liu, J. Chem. Phys. **119**, 2538 (2003).
[130] J. Zhou, J. J. Lin, and K. Liu, J. Chem. Phys. **119**, 8289 (2003).
[131] W. Shiu, J. J. Lin, K. Liu, M. Wu, and D. H. Parker, J. Chem. Phys. **120**, 117 (2004).
[132] W. Shiu, J. J. Lin, and K. Liu, Phys. Rev. Lett. **92**, 103201 (2004).
[133] J. Zhou, W. Shiu, J. J. Lin, and K. Liu, J. Chem. Phys. **120**, 5863 (2004).
[134] D. M. Neumark, A. M. Wodtke, G. N. Robinson, C. C. Hayden, K. Shobatake, R. K. Sparks, T. P. Schafer, and Y. T. Lee, J. Chem. Phys. **82**, 3067 (1985).
[135] J. Zhou, J. J. Lin, K. Liu, J. Chem. Phys, **121**, 813 (2004).
[136] F. Dong, S. H. Lee, and K. Liu, J. Chem. Phys. **113**, 3633 (2000).
[137] W. W. Harper, S. A. Nizkorodov, and D. J. Nesbitt, J. Chem. Phys. **116**, 5622 (2002)
[138] W. W. Harper, S. A. Nizkorodov, and D. J. Nesbitt, J. Chem. Phys. **113**, 3670 (2000).
[139] W. W. Harper, S. A. Nizkorodov, and D. J. Nesbitt, Chem. Phys. Lett. **335**, 381 (2001).
[140] E. S. Whitney, A. Zolot, A. B. McCoy, J. S. Francisco, and D. J. Nesbitt, private communication (2004).
[141] H. Kornweitz, A. Persky, and R. D. Levine, Chem. Phys. Lett. **289**, 125 (1998).
[142] K. Sugawara, F. Ito, T. Nakanaga, H. Takeo, and C. Matsumura, J. Chem. Phys. **92**, 5328 (1990).
[143] R. Atkinson, D. L. Baulch, R. A. Cox, R. F. Hampson Jr, J. A. Kerr, M. J. Rossi, and J. Troe, J. Phys. Chem. Ref. Data. **26**, 521 (1997).
[144] S. P. Sander, B. J. Finlayson-Pitts, R. R. Friedl, D. M. Golden, R. E. Huie, C. E. Kolb, M. J. Kurylo, M. J. Molina, G. K. Moortgat, V. L. Orkin, and A. R. Ravishankara, Chemical Kinetics and Photochemical Data for Use in Atmospheric Studies, Evaluation Number 14. JPL Publication 02-25, Jet Propulsion Laboratory, Pasadena (2002).
[145] J. V. Michael, D. F. Nava, W. A. Payne, and L. J. Stief, J. Chem. Phys. **70**, 3652 (1979).

[146] W. A. Payne, J. Brunning, M. B. Mitchell, and L. J. Stief, Int. J. Chem. Kinet, **20**, 63 (1988).
[147] J. T. Jodkowski, M.-T. Rayez, J.-C. Rayez, T. Bérces, and S. Dóbé, J. Phys. Chem. A. **102**, 9230 (1998).
[148] C. Kollias, O. Couronne, and W. A. Lester Jr, J. Chem. Phys. **121**, 1357 (2004).
[149] J. D. Smith, J. D. DeSain, and C. A. Taatjes, Chem. Phys. Lett. **366**, 417 (2002).
[150] P. W. Seakins, J. J. Orlando, and G. S. Tyndall, Phys. Chem. Chem. Phys. **6**, 2224 (2004).
[151] C. A. Taatjes, L. K. Christensen, M. D. Hurley, and T. J. Wallington, J. Phys. Chem. A, **103**, 9805 (1999).
[152] S. Rudić, C. Murray, D. Ascenzi, H. Anderson, J. N. Harvey, and A. J. Orr-Ewing, J. Chem. Phys. **117**, 5692 (2002).
[153] W. S. Goliff, and F. S. Rowland, Geophys. Res. Lett. **24**, 3029 (1997).
[154] S. M. A. Hoffmann, D. J. Smith, A. González-Ureña, and R. Grice, Chem. Phys. Lett. **107**, 99 (1984).
[155] C. A. Piety, R. Soller, J. M. Nicovich, M. L. McKee, and P. H. Wine, Chem. Phys. **231**, 155 (1998).
[156] Y. V. Ayhens, J. M. Nicovich, M. L. McKee, and P. H. Wine, J. Phys. Chem. A. **101**, 9382 (1997).
[157] M.-T. Rayez, J.-C. Rayez, and J.-P. Sawerysyn, J. Phys. Chem. **98**, 11342 (1994).
[158] E. Rosenman, and M. L. McKee, J. Am. Chem. Soc. **119**, 9033 (1997).
[159] J.-F. Xiao, Z.-S. Li, Y.-H. Ding, J.-Y. Liu, X.-R. Huang, and C.-C. Sun, Phys. Chem. Chem. Phys. **3**, 3955 (2001).
[160] S. Rudić, D. Ascenzi, and A. J. Orr-Ewing, Chem. Phys. Lett. **332**, 487 (2000).
[161] H. A. Bechtel, J. P. Camden, and R. N. Zare, J. Chem. Phys. **120**, 4231 (2004).
[162] S. Rudić, C. Murray, J. N. Harvey, and A. J. Orr-Ewing, Phys. Chem. Chem. Phys. **5**, 1205 (2003).
[163] C. S. Kegley-Owen, G. S. Tyndall, J. J. Orlando, and A. Fried, Int. J. Chem. Kinet. **31**, 766 (1999).
[164] J. A. Beukes, B. D'Anna, V. Bakken, and C. J. Nielsen, Phys. Chem. Chem. Phys. **2**, 4049 (2000).
[165] F. Dong, Z. Qu, Q. Zhang, and F. Kong, Chem. Phys. Lett. **371**, 29 (2003).
[166] S.-S. Cheng, Y.-J. Wu, and Y.-P. Lee, J. Chem. Phys. **120**, 1792 (2004).
[167] D. J. Nesbitt, and S. R. Leone, J. Chem. Phys. **75**, 4949 (1981).
[168] B. Dill, and H. Heydtmann, Chem. Phys. Lett. **35**, 161 (1978).
[169] C. Wilson, and D. M. Hirst, J. Chem. Soc. Faraday Trans. **93**, 2831 (1997).
[170] T. A. Steele, N. Bradshaw, and R. Grice, J. Chem. Soc. Faraday Trans. 2. **82**, 631 (1986).
[171] M. Ahmed, D. S. Peterka, and A. G. Suits, Chem. Phys. Lett. **317**, 264 (2000).
[172] M. Ahmed, D. S. Peterka, and A. G. Suits, Phys. Chem. Chem. Phys. **2**, 861 (2000).
[173] C. Murray, A. J. Orr-Ewing, R. L. Toomes, and T. N. Kitsopoulos, J. Chem. Phys. **120**, 2230 (2004).
[174] R. L. Toomes, A. J. van den Brom, T. N. Kitsopoulos, C. Murray, and A. J. Orr-Ewing, J. Phys. Chem. A. **108**, 7909 (2004).
[175] R. E. Miller, private communication (2004).
[176] S. S. Parmar, and S. W. Benson, J. Am. Chem. Soc. **111**, 57 (1989).